Journal of Medicinal Chemistry

Article

Novel Tetrazole-containing Analogs of Itraconazole as Potent Anti-angiogenic Agents with Reduced CYP3A4 Inhibition

Yingjun Li, Kalyan Kumar Pasunooti, Ruo-Jing Li, Wukun Liu, Sarah A. Head, Wei Q. Shi, and Jun O. Liu

J. Med. Chem., **Just Accepted Manuscript** • DOI: 10.1021/acs.jmedchem.8b01252 • Publication Date (Web): 27 Nov 2018

Just Accepted

ACS Publications

is published by the American Chemical Society. 1155 Sixteenth Street N.W., Washington, DC 20036

Novel Tetrazole-containing Analogs of Itraconazole as Potent Anti-angiogenic Agents with Reduced CYP3A4 Inhibition

Yingjun Li[†,II] Kalyan Kumar Pasunooti,[†,II] Ruo-Jing Li,[†] Wukun Liu,[†] Sarah A. Head,[†] Wei Q. Shi,[†] Jun O. Liu*[, †, ‡]

[†]Department of Pharmacology and Molecular Sciences, Johns Hopkins School of Medicine, Baltimore, Maryland 21205, United States

[‡]Department of Oncology, Johns Hopkins School of Medicine, Baltimore, Maryland 21205, United States

[II] These authors contributed equally to this work.

Corresponding Author

*J.O.L.: phone, 410-955-4619; fax, 410-955-4520; e-mail, joliu@jhu.edu

ABSTRACT

Itraconazole has been found to possess potent anti-angiogenic activity, exhibiting promising antitumor activity in several human clinical studies. The wider use of itraconazole in the treatment of cancer, however, has been limited by its potent inhibition of the drug metabolizing enzyme CYP3A4. In an effort to eliminate the CYP3A4 inhibition while retaining its anti-angiogenic activity, we designed and synthesized a series of derivatives in which the 1, 2, 4-triazole ring is replaced with various azoles and non-azoles. Among these analogs, **15n** with tetrazole in place of 1, 2, 4-triazole exhibited optimal inhibition of HUVEC proliferation with an IC_{50} of 73 nM without significant effect on CYP3A4 ($EC_{50} > 20$ μM). Similar to itraconazole, **15n** induced Nieman-Pick C phenotype (NPC phenotype) and blocked AMPK/mTOR signaling. These results suggest that **15n** is a promising angiogenesis inhibitor that can be used in combination with most other known anticancer drugs.

Introduction:

Angiogenesis, the formation of new blood vessels, plays a critical role in the onset and progression of cancer as well as a number of other human diseases.[1] Inhibition of angiogenesis has become an important strategy to combat cancer as underscored by the clinical introduction of a number of inhibitors of angiogenesis.[2] In an effort to repurpose existing drugs as new angiogenesis inhibitors, we previously found that the antifungal drug itraconazole (**1,** Fig. 1) possessed potent anti-angiogenic activity.[3,4] The molecular target of itraconazole underlying its antifungal activity is lanosterol 14α-demethylase (14-DM).[5] However, itraconazole only shows weak inhibition of human 14-DM, ruling it out as a relevant target for the anti-angiogenic activity of itraconazole.[6] Instead, we have identified voltage-dependent anion channel (VDAC)1 and Niemann Pick type C (NPC)1 as direct targets of itraconazole.[7,8,9] We have shown that binding of itraconazole to NPC1 leads to inhibition of cholesterol trafficking out of the endolysosome, which in turn induces NPC1 phenotype. Binding of itraconazole to VDAC1 blocks ATP biosynthesis in the mitochondria, increasing cytosolic AMP/ATP ratio and activating AMPK. Inhibition of cholesterol trafficking and activation of AMPK lead to synergistic inhibition of mTOR signaling.[10] The unique mechanism of action of itraconazole distinguishes it from rapamycin, a direct inhibitor of mTOR, and other azole antifungal drugs such as ketoconazole (**2,** Fig. 1), which do not have antiangiogenic activity.[11] These new mechanistic insights, along with other preclinical results, have facilitated the entrance of itraconazole into multiple phase II clinical trials in the treatment of prostate cancer, non-small cell lung cancer, basal cell carcinoma and other types of cancers.[12,13,14,15]

A major limitation of itraconazole as a novel anticancer drug is its strong inhibition of human liver cytochrome P450 3A4 (CYP3A4).[16] CYP3A4 is a major xenobiotic metabolizing enzyme and it contributes to the metabolism of approximately 50% of prescribed drugs, including the majority of anticancer drugs.[17] Inhibition of CYP3A4 causes strong drug-drug interaction, preventing the combination of itraconazole with most known anticancer drugs including targeted kinase inhibitors that are metabolized by CYP3A4.[18,19] Many anticancer drugs, especially those that inhibit angiogenesis, are most effective when used in combination with other drugs.[20] Thus, there is a need to develop novel itraconazole analogs with reduced or with no CYP3A4 inhibition while retaining its anti-angiogenic activity.

Previously, we identified an itraconazole stereoisomer with *cis-2S,4R* stereochemistry of the dioxolane moiety with increased anti-angiogenic activity and significantly reduced hepatotoxicity.[21,22] We also found that the *sec*-butyl or a similar side chain is required for antiangiogenic activity.[23] The triazole moiety of itraconazole is a critical pharmacophore required for the binding of itraconazole to the heme group of 14-DM as well as the heme group of CYP3A4.[24,25] However, little is known about the importance of the triazole moiety in anti-angiogenic activity of itraconazole.[26]

In an effort to identify novel analogs of itraconazole with reduced or no CYP3A4 inhibition while retaining its anti-angiogenic potency, we systematically replaced the 1,2,4-triazole moiety with different non-azoles or azoles. Herein, we report the SAR (structure–activity relationship) study of novel itraconazole analogs for their anti-angiogenic activity and CYP3A4 inhibition. Further, we identified one compound, **15n**, which contains tetrazole in place of triazole and exhibits improved anti-angiogenic activity and significantly reduced CYP3A4 inhibitory activity compared with itraconazole.

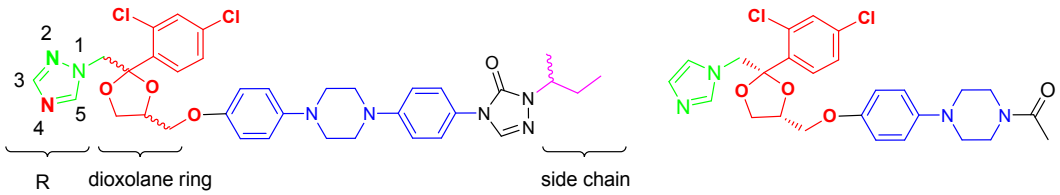

Figure 1. Structures of itraconazole (**1**) and ketoconazole (**2**).

Results and Discussion

Chemistry:

The synthetic route to the non-azole itraconazole analogs (**10a-10e**) is outlined in Scheme 1. The synthesis commenced with the commercially available 1, 3-dichlorobenzene and a series of different acid chlorides. The intermediates 2, 4-dichloro benzaldehyde (**5a**) and 2-bromo-2',4'-dichloroacetophenone (**5c**) are commercially available. The other intermediates (**5b, 5d and 5e)** were efficiently prepared by the acylation of 1, 3-dichlorobenzene with acid chlorides under Friedel-Craft acylation conditions in satisfactory yields (70-90%). Our previous results

suggested that *2S,4R-cis*-stereochemistry on the 1, 3-dioxalane ring is more potent for anti-angiogenic activity than alternative stereochemical configurations.[21] We thus constructed the *cis*-1,3-dioxolane (**7a-7e**) *via* acid-assisted ketalization of 2, 4-dichloro acetophenones (**5a-5e**) with optically pure glyceryl tosylate **6** in the presence of trifluoromethanesulfonic acid (TfOH) in toluene, yielding *cis* and *trans* diastereomers in the ratio of 3:1 with good yields. Those two diastereomers were separated by conventional column chromatography. The required phenol fragment **9** was synthesized with the same method as we reported previously.[23] The phenol fragment **9** was reacted with the O-tosylates (**7a-7e**) in the presence of sodium hydride (NaH) to afford final products (**10a-10e**). Analogs with a tertiary amine group (**11a-11d**) were prepared from a nucleophilic substitution reaction of bromo substituted compound **10c** with different secondary amines (Scheme 2).

Itraconazole analogs (**15a-15q**) were synthesized using a similar route (Scheme 3). The intermediates **12a-12q** were prepared by N-alkylation of 2-bromo-2',4'-dichloroacetophenone (**5c**) with a series of azoles in DCM at room temperature. Ketalization of 2, 4-dichloro acetophenones **12a-12q** with glyceryl tosylate **6** gave **13a-13q** as *cis* diastereoisomers with low to moderate yields (10% - 65%). Finally, O-tosylates (**13a-13q**) were treated with fragment **9** to yield the desired products **15a-15q**.[27]

Scheme 1:

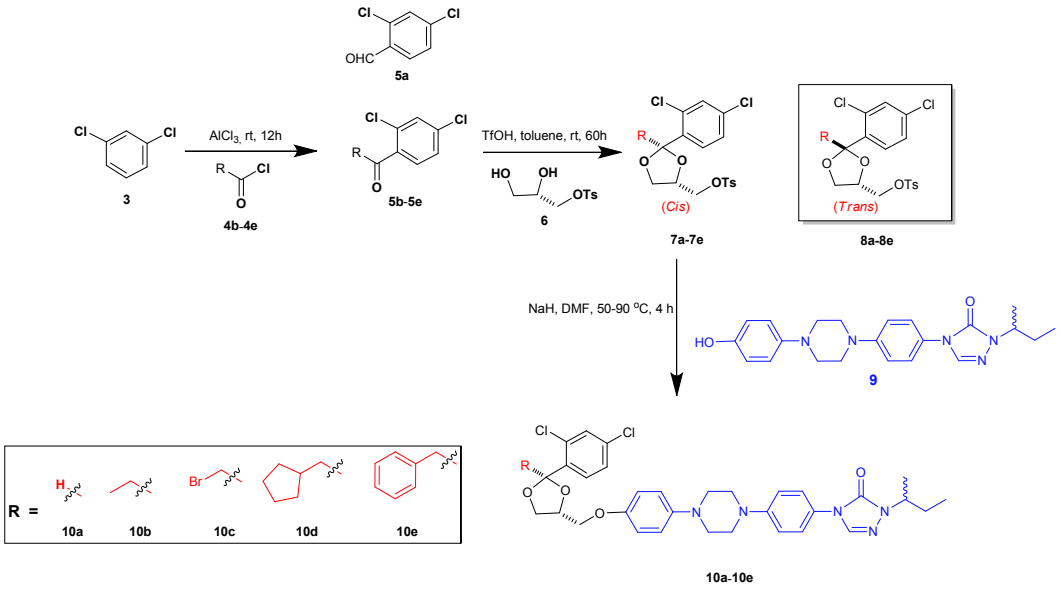

Scheme 2:

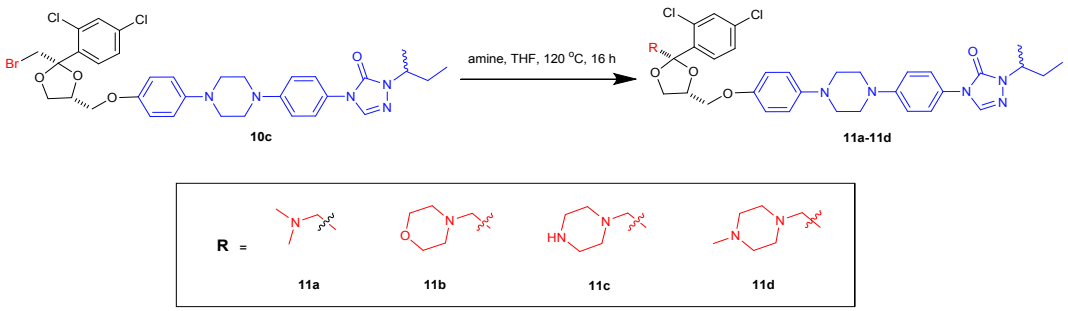

Scheme 3:

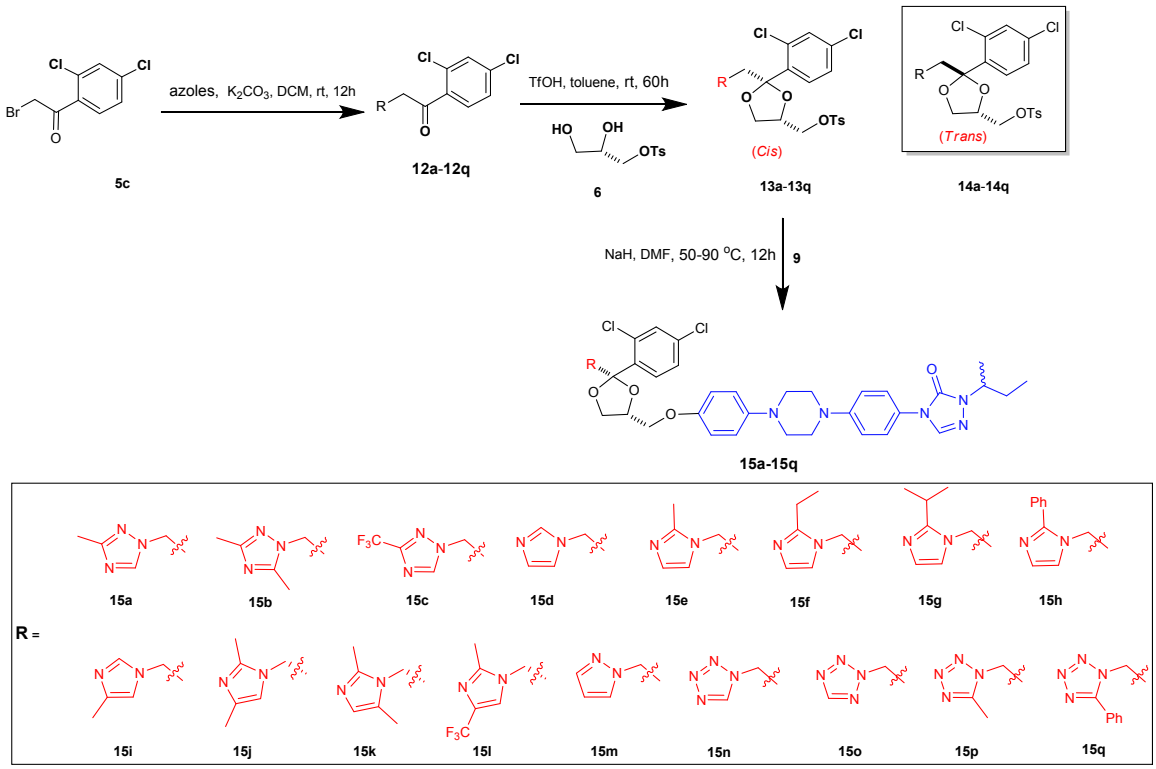

SAR studies of new itraconazole analogs using HUVEC proliferation and CYP3A4 enzymatic assays

The anti-angiogenic activity of new itraconazole analogs was determined using HUVEC proliferation assay with [^{3}H] thymidine incorporation as a readout (Table 1).[3] CYP3A4 inhibition was determined using a cell-free fluorescence-based assay at 1 μM of each analog after concentration optimization of itraconazole (Fig. S1).[28]

To assess the importance of the triazole moiety for the anti-angiogenic activity of itraconazole and CYP3A4 inhibition, we removed the 1,2,4-triazolyl-methyl group (**10a**) or replaced it with ethyl (**10b**), bromo methyl (**10c**), cyclopentyl-methyl (**10d**), or phenyl-methyl group (**10e**). As expected, **10a-10e** without a nitrogen atom in the R position exhibited no CYP3A4 inhibition at 1 μM. Further dose response assays showed that **10b** completely lost CYP3A4 inhibition (Fig. 2). In contrast, the same group of analogs only suffered a 2-3 fold decrease in anti-proliferative activity against HUVEC, suggesting differential dependence of the two activities on the presence of the triazole moiety.

Next, a tertiary amine was introduced to 1,2,4-triazole position (**11a-11d**) with dimethylamine, morpholine, piperidyl or N-methyl piperidyl group, respectively. Analogs **11a-11d** have the added advantage of having improved water solubility compared with itraconazole. The analogs containing an aliphatic amine in place of 1,2,4-triazole inhibited CYP3A4 at 1 μM except for **11a**. Structurally, **11b-11d** have a nucleophilic nitrogen atom or oxygen atom in a position comparable to N4 of 1,2,4-triazole in itraconazole, suggesting that the aliphatic nitrogen and oxygen are also capable of interacting with the heme group in CYP3A4. Compared to itraconazole, **11a-11d** had a 2-9 fold decrease in anti-proliferative activity in HUVEC. Together, the results confirmed that CYP3A4 inhibition of itraconazole is highly dependent on 1,2,4-triazole moiety, in particular the basic N4 atom of triazole and suggested that replacing the triazole moiety with non-azoles is not sufficient to decrease CYP3A4 inhibition without compromising the anti-angiogenic activity.

Given the importance of the triazole moiety in the anti-angiogenic activity of itraconazole, we decided to make less drastic structural alterations of the triazole by increasing the steric hindrance around the nitrogen atom at 4 position that might decrease its access to the heme iron in CYP3A4. To start with, we introduced methyl or trifluoromethyl substitution on 1,2,4-triazole ring. Analogs **15a** with 3-methyl-1*H*-1,2,4-triazole substitution and **15b** with 3,5-dimethyl-1*H*-1,2,4-triazole substitution showed reduced potency in CYP3A4 inhibition. The trifluoromethyl substituted compound **15c** showed no CYP3A4 inhibition at 1 μM and weak inhibition at higher concentrations (Fig. 2). The IC_{50} values of **15a-15c** for inhibition of HUVEC proliferation were 0.27, 0.22, and 0.27 μM, respectively, slightly higher than that of itraconazole (0.17 μM). Compound **15d** contains an imidazole in place of the 1,2,4-triazole

and exhibited higher potency against HUVEC proliferation than itraconazole. We synthesized a series of analogs containing imidazole group with various substitutions (**15e**-**15l**). Similar to **15c**, compound **15l** with 2-methyl-4-trifluoromethyl-1*H*-imidazol-yl moiety suffers from both steric hindrance and electron withdrawing effect exerted by the trifluoromethyl group, rendering the N3 nitrogen unreactive towards heme. As expected, 15l had no inhibitory effect on CYP3A4 at 1 μM. However, the dual substituted compounds (**15j**-**15l**) also suffered a 2-3 fold decrease in anti-angiogenic activity. Interestingly, among the single substituted imidazol-yl compounds, the 2-isopropyl-1*H*-imidazol-yl analog **15g** had the most potent HUVEC inhibition activity, with an IC_{50} of 0.084 μM. Compounds with substituents smaller or larger than the isopropyl group were all less potent than **15g**. On the other hand, CYP3A4 inhibition showed an opposite trend—the larger the substituents on the imidazole, the less inhibition of CYP3A4.

As coordination of the basic nitrogen to heme iron is required for the inhibitory activity of azoles against CYP3A4, we reasoned that replacement of triazole with tetrazole that has reduced basicity compare to imidazole and triazole, should has reduced CYP3A4 inhibition.[29] The 1-tetrazole-yl analog **15n** showed improved anti-proliferative activity in HUVEC with an IC_{50} of 0.073 μM and significantly reduced CYP3A4 inhibition with an EC_{50} above 20 μM (Fig. 2). In contrast, the structurally related 2-tetrazole-yl analog **15o** is less potent in HUVEC and exhibited greater CYP3A4 inhibition than **15n**. Addition of a 5-methyl or 5-phenyl substituents to the tetrazole group did not lead to further improvement over analog **15n**, rendering **15n** the optimal compound among all itraconazole analogs made to date. Thus, we selected **15n** for further biological evaluation.

Inhibition of Tube Formation

To further assess the anti-angiogenic activity of **15n**, we employed an *in vitro* tube formation assay. In this assay, HUVEC were seeded on matrigel, cells migrate and elongate to form tubule-like networks after 20 hours, which is reminiscent of new blood vessel formation.[30] As showed in Fig. 3, treatment of HUVEC with 5 μM itraconazole inhibited 45% of HUVEC tube formation as judged by the total tube length. At the same concentration, **15n** inhibited 61% of HUVEC tube formation, confirming that **15n** is a more potent anti-angiogenesis inhibitor.

Table 1: HUVEC Anti-proliferation Activities and CYP3A4 Enzyme Inhibition of Itraconazole Analogs

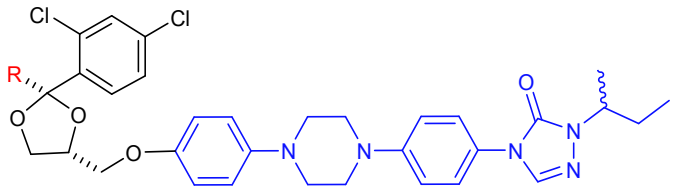

Compounds	R	HUVEC IC_{50} (μM) [a]	CYP3A4 inhibition at 1μM [b]
1		0.170 ± 0.013	84% ± 6%
10a	H	0.328 ± 0.070	NI
10b		0.353 ± 0.033	NI
10c		0.569 ± 0.200	3% ± 1%
10d	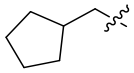	0.512 ± 0.177	NI [c]
10e	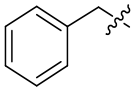	0.513 ± 0.125	NI
11a		1.397 ± 0.165	NI
11b	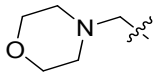	1.175 ± 0.231	16% ± 3%
11c	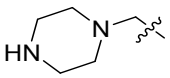	0.608 ± 0.260	91% ± 1%
11d	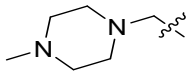	0.396 ± 0.168	18% ± 7%
15a	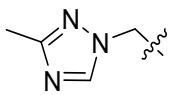	0.272 ± 0.112	30% ± 7%
15b	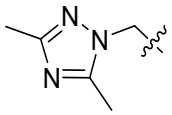	0.221 ± 0.008	27% ± 4%
15c	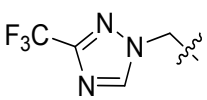	0.270 ± 0.084	NI
15d	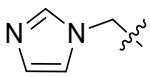	0.085 ± 0.014	99% ± 1%

15e	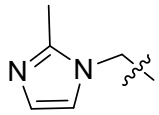	0.173 ± 0.063	71% ± 13%
15f	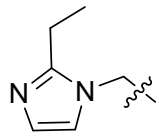	0.224 ± 0.064	7% ± 4%
15g	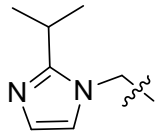	0.084 ± 0.016	6% ± 3%
15h	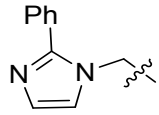	0.136 ± 0.070	23% ± 11%
15i	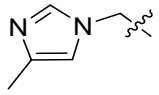	0.102 ± 0.015	98% ± 2%
15j	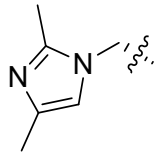	0.492 ± 0.053	38% ± 4%
15k	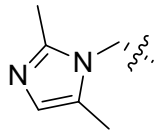	0.765 ± 0.072	23% ± 7%
15l	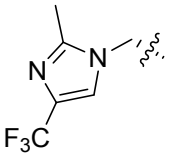	0.441 ± 0.134	NI
15m	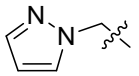	0.307 ± 0.045	NI
15n	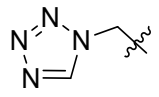	0.073 ± 0.017	2% ± 1%
15o	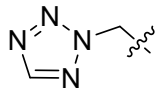	0.124 ± 0.049	17% ± 4%
15p	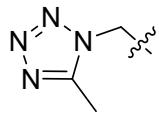	0.101 ± 0.047	7% ± 5%
15q	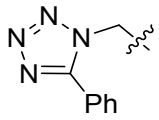	0.119 ± 0.011	18% ± 5%

[a] IC_{50} in HUVEC were evaluated using 3H thymidine incorporation assay. [b] CYP3A4 enzyme inhibition was evaluated using Vivid® CYP3A4 green screening assay. Values indicated are % enzyme inhibition at 1 µM. Values represent the mean ± SD in three independent experiments carried out in triplicate. [c] No Inhibition.

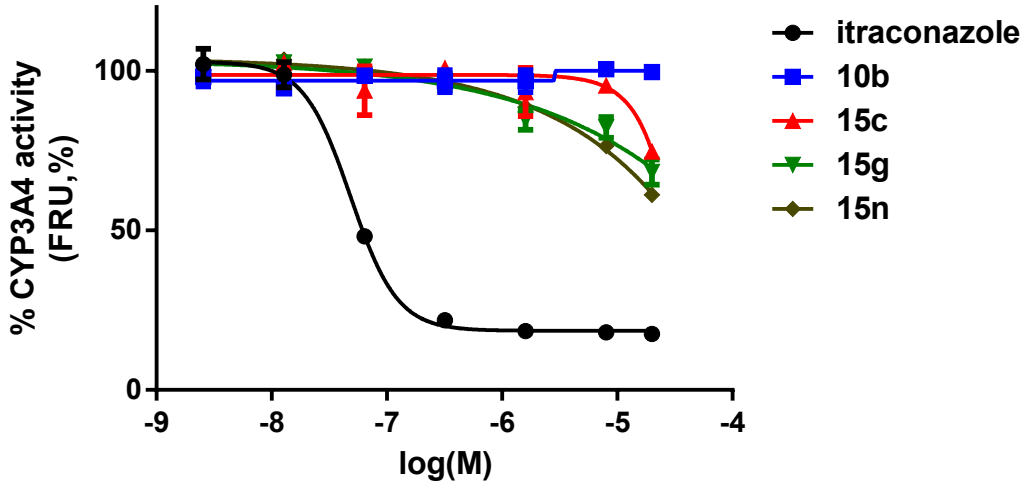

Figure 2. CYP3A4 enzyme activity in the presence of different concentrations of itraconazole (**1**), **10b**, **15c**, **15g** and **15n**.

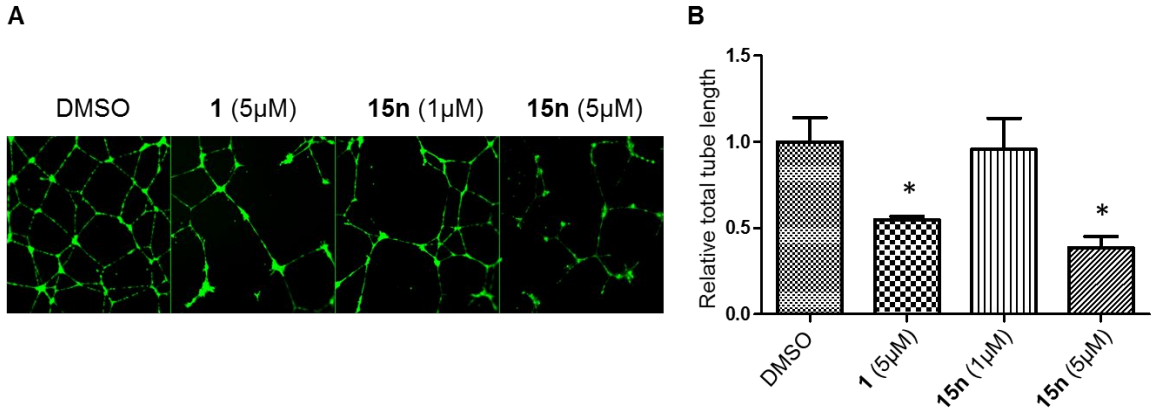

Figure 3. Compound **15n** inhibits HUVEC tube formation. HUVECs were plated on Matrigel and treated with 5µM itraconazole (**1**), 1µM **15n**, 5µM **15n** or DMSO for 20h. (**A**) Cells were stained with Calcein-AM and vascular networks were imaged using fluorescence microscopy. (**B**) Total tube lengths from the fluorescence images were quantified using the ImageJ software and plotted using GraphPad Prism. Data, mean ± SD of three independent experiments. (* $p <$ 0.01)

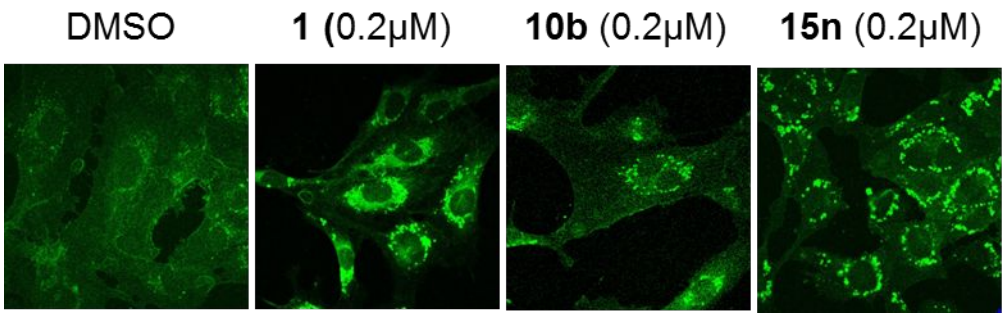

Figure 4. Itraconazole (**1**), **10b** and **15n** induce NPC phenotype at 0.2μM. HUVECs were treated with 0.2 μM itraconazole (**1**), 0.2 μM **15n** or DMSO for 24 h. Intracellular cholesterol was visualized using filipin staining and fluorescent images were captured under a confocal microscope.

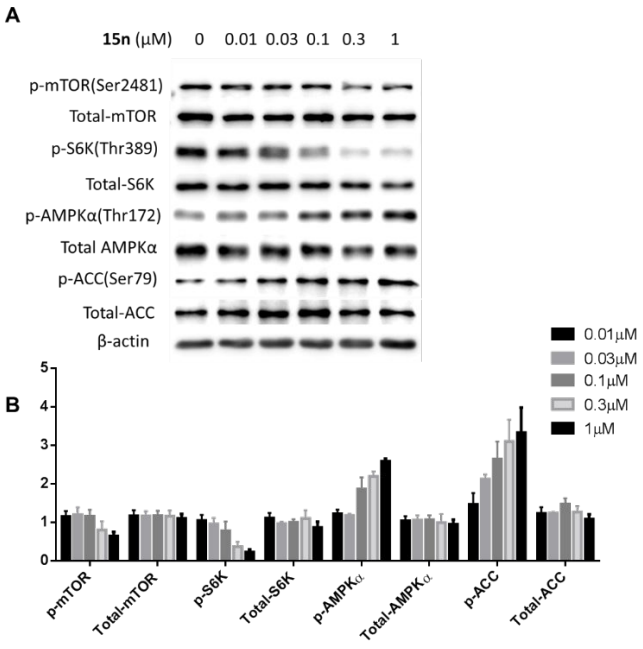

Figure 5. 15n dose-dependently activates AMPKα and inhibits mTOR in HUVECs. (**A**) HUVECs were treated with 0.01μM, 0.03μM, 0.1μM, 0.3μM, 1μM of **15n** or DMSO for 24 h. Cell lysates were subjected to Western Blot. (**B**) The mean gray value and area of the blots were quantified using the ImageJ software and plotted using GraphPad Prism. Data given as mean ± SD of three independent experiments.

Nieman-Pick C phenotype and mTOR inhibition

We have previously shown that the mechanism underlying the anti-angiogenic activity of itraconazole is mediated in part through inhibition of endolysosomal cholesterol trafficking and mTOR inhibition. We thus determined whether compound **15n** shared the same mechanism with itraconazole. Intracellular cholesterol was detected using the cholesterol-binding fluorescent dye filipin.[10] Similar to itraconazole, **15n** induced NPC phenotype at a concentration of 0.2 μM as judged by the accumulation of cholesterol in the late endosome/lysosome (Fig. 4). Compound **10b**, which was less potent against HUVEC, showed reduced activity in NPC phenotype induction. Other compounds **15c** and **15g** also induced cholesterol accumulation (Fig. S2). Analog **15n** also increased the phosphorylation of the α subunit of AMPK at Thr172 in a dose-dependent manner (Fig. 5). The phosphorylation of the AMPK substrate acetyl CoA carboxylase 1 (ACC1) was also increased as expected.[31,32] In addition, treatment of HUVEC with **15n** led to a decrease in the phosphorylation of mTOR and its substrate p70 S6 Kinase (S6K). A significant change was seen in AMPK signaling at 0.1μM of **15n** and in mTOR signaling at 0.3μM of **15n** (Fig. 5B, Fig. S3). Moreover, pretreatment with **15h** and **15n** was able to compete the crosslinking of the itraconazole photoaffinity probe (Fig. S5) to VDAC1 similar to itraconazole (Fig. S4), indicating direct binding of **15h** and **15n** to VDAC1. Together, these results suggested that **15n** inhibited HUVEC proliferation and angiogenesis with the same targets and underlying mechanism as itraconazole.

Conclusions

The antifungal drug was identified and validated as a promising anti-angiogenic agent, demonstrating efficacy against different types of cancer in multiple Phase 2 human clinical studies. The inhibition of CYP3A4 by itraconazole, however, severely limits its wider use as an anticancer agent due to interactions with most other known anticancer drugs. To overcome this limitation, we have synthesized a series of azole and non-azole derivatives of itraconazole in attempts to maintain their anti-angiogenic activity while reducing or eliminating their effects on CYP3A4. Given that the CYP3A4 inhibition is highly dependent on the coordination of 1,2,4-triazole to the heme iron in CYP3A4, we carried out a series of chemical modifications of triazole moiety to reduce binding of itraconazole analogs to CYP3A4. In addition to

replacing the triazole with alkyl or alkylamine substituents, we also incorporated methyl and trifluoromethyl substituents to azoles to decrease the azole-heme iron interaction through steric hindrance or reduction of basicity of the azole nitrogen. While many of the analog showed significantly reduced or no inhibition of CYP3A4, their inhibitory activity against HUVEC was also decreased in comparison to itraconazole. Eventually, we attempted to replace triazole with tetrazole and one of the analogs, **15n,** not only has significantly reduced CYP3A4 inhibition with an EC_{50} of above 20 μM, but also exhibited more potent anti-proliferative activity against HUVEC than itraconazole. The angiogenic potency of **15n** was further confirmed by HUVEC tube formation. Like itraconazole, **15n** bound to VDAC1 as judged by its competition for VDAC1 binding against the itraconazole photoaffinity probe, activated AMPK pathway, induced NPC1 phenotype and inhibited mTOR, which are hallmarks of the mechanism of inhibition of angiogenesis by itracoazole. Together, our results strongly suggest that the tetrazole-containing analog **15n** is a promising new lead for the development of the next generation itraconazole analogs that can be used in combination with most other known anticancer drugs.

Experimental Section:

Chemistry. Reactions were carried out in oven-dried glassware. All reagents were purchased from commercial sources and were used without further purification unless noted. Unless otherwise stated, all reactions were carried out under argon atmosphere, monitored by Merck pre-coated silica gel 60F-254 plates and visualized using 254 nm UV light. Column chromatography was performed on normal-phase silica flash columns (RediSepRf). NMR data were collected on Bruker Avance III (500 MHz ^{1}H, 125 MHz ^{13}C) machine in the Department of Pharmacology and Molecular Sciences, the Johns Hopkins University, School of Medicine. Chemical shifts (δ) are reported in ppm. ^{1}H NMR spectra and ^{13}C NMR spectra were obtained in deuteriochloroform ($CDCl_3$) with tetramethylsilane (TMS, δ = 0.00 for ^{1}H) as an internal reference. Data are presented in the form: chemical shift (multiplicity, coupling constants, and integration). Low resolution ESI-MS and HPLC purity were recorded on an Agilent 6120 quadrupole LC/MS. The reported purity values were obtained with a Pursuit XRs Diphenyl

column (150×4.5mm) and a diode array detector (DAD). A flow rate of 1.0 ml/min was used with a mobile phase of solvent A (H_2O with a 0.1% formic acid (v/v)) and solvent B (acetonitrile with a 0.1% formic acid (v/v)). A gradient elution method were used: started with 40% solvent B, changed to 95% over 14 min, maintained at 95% for 3min and then change to 40% over 0.5 min, maintained at 40% for 2.5 min. The absorbance was detected under UV at 250nm and area of peaks were quantified to calculate the compound purity. The purity of all compounds are ⩾95%.

General experimental procedure for 10a-10e and 15a-15q

To a solution of tosylates **7a-7e** and **13a-13q** (1 eq) in anhydrous DMF was added sodium hydride (NaH, 60% dispersion in mineral oil, (1.5 eq) under argon atmosphere. After tiring at 50℃ for 1 hour, a solution of **9** (1.2 eq) in DMF was added slowly at the same temperature. Then the temperature was increased to 90℃ and the reaction was stirred for another 3 hours. The reaction mixture was quenched by the saturated sodium chloride, and the resulting mixture was extracted twice with dichloromethane. The organic fractions were dried over Na_2SO_4, filtered and concentrated under vacuum to yield the crude product which was purified by column chromatography to afford the desired product **10a-10e** and **15a-15q** in moderate to good yields.

1-*sec*-butyl-4-(4-(4-(4-(((*4R*)-2-(2,4-dichlorophenyl)-1,3-dioxolan-4-yl)methoxy)phenyl)piperazin-1-yl)phenyl)-1*H*-1,2,4-triazol-5(4*H*)-one (Mixture of trans and cis) (10a). Trans compound: ^{1}H NMR (500 MHz, $CDCl_3$, δ_H): 7.62 (s, 1H), 7.57 (d, *J* = 8.5 Hz, 1H), 7.43 (d, *J* = 8.5 Hz, 2H), 7.40 (t, *J* = 2.0 Hz, 1H), 7.28 (t, *J* = 2.0 Hz, 1H), 7.27(bs, 1H), 7.03 (d, *J* = 9.0 Hz, 2H), 6.95 (bs, 1H), 6.92-6.88 (m, 2H), 6.27 (s, 1H), 4.66-4.60 (m, 1H), 4.34 (dd, *J* = 8.2, 6.7 Hz, 1H), 4.31-4.27 (m, 1H), 4.18-4.15 (m, 1H), 4.14-4.07 (m, 1H), 4.03 (dd, *J* = 8.5, 6.5 Hz, 1H), 3.37 (bs, 4H), 3.25 (bs, 4H), 1.90 – 1.84 (m, 1H), 1.75 – 1.69 (m, 1H), 1.39 (d, *J* = 6.5 Hz, 3H), 0.91 (t, *J* = 7.2 Hz, 3H). ^{13}C NMR (125 MHz, $CDCl_3$, δ_C): 152.1, 135.8, 135.7, 134.4, 134.3, 133.9, 129.6, 128.8, 127.4, 127.2, 123.6, 118.5, 116.7, 115.5, 100.7, 76.5, 74.7, 68.7, 68.6, 67.9, 52.7, 50.7, 28.5, 19.3, 10.8. Cis compound: ^{1}H NMR (500 MHz, $CDCl_3$, δ_H): 7.62 (s, 1H), 7.57 (d, *J* = 8.5 Hz, 1H), 7.43 (d, *J* = 8.5 Hz, 2H), 7.40 (t, *J* = 2.0 Hz, 1H), 7.29 (d, *J* = 2.0 Hz, 1H), 7.27(bs, 1H), 7.03 (d, *J* = 9.0 Hz, 2H), 6.95 (bs, 1H), 6.92-6.88 (m, 2H), 6.16 (s, 1H), 4.66-4.60 (m, 1H), 4.31-4.27 (m, 1H), 4.21 (dd, *J* = 8.2, 6.7

Hz, 1H), 4.18-4.15 (m, 1H), 4.14-4.07 (m, 1H), 4.03 (dd, *J* = 8.5, 6.5 Hz, 1H), 3.37 (bs, 4H), 3.25 (bs, 4H), 1.90 – 1.84 (m, 1H), 1.75 – 1.69 (m, 1H), 1.39 (d, *J* = 6.5 Hz, 3H), 0.91 (t, *J* = 7.2 Hz, 3H). ^{13}C NMR (125 MHz, $CDCl_3$, δ_C): 152.1, 135.8, 135.7, 134.4, 134.3, 133.9, 129.6, 128.8, 127.4, 127.2, 123.6, 118.5, 116.7, 115.5, 100.7, 76.5, 74.7, 68.7, 68.6, 67.9, 52.7, 50.7, 28.5, 19.3, 10.8. HRMS (ESI) calcd for $C_{32}H_{35}Cl_2N_5O_4$: 624.2144; found 624.2114. HPLC Purity: 95.9%, tR = 13.7 min.

1-*sec*-butyl-4-(4-(4-(4-(((*2R,4R*)-2-(2,4-dichlorophenyl)-2-ethyl-1,3-dioxolan-4-yl)methoxy)phenyl)piperazin-1-yl)phenyl)-1*H*-1,2,4-triazol-5(4*H*)-one (10b). ^{1}H NMR (500 MHz, $CDCl_3$, δ_H): 7.61 (s, 1H), 7.57 (d, *J* = 8.0 Hz, 1H), 7.43 (d, *J* = 9.0 Hz, 2H), 7.40 (d, *J* = 2.0 Hz, 1H), 7.23 (dd, *J* = 8.5, 2.0 Hz, 1H), 7.03 (d, *J* = 9.0 Hz, 2H), 6.95 (bs, 2H), 6.89 (d, *J* = 9.0 Hz, 2H), 4.33-4.27 (m, 2H), 4.12 (dd, *J* = 9.5, 5.0 Hz, 1H), 3.98 (dd, *J* = 8.5, 4.5 Hz, 1H), 3.96 (dd, *J* = 9.5, 6.5 Hz, 1H), 3.86 (dd, *J* = 8.5, 7.0 Hz, 1H), 3.37 (bs, 4H), 3.24 (bs, 4H), 2.18 – 2.09 (m, 2H), 1.89 – 1.83 (m, 1H), 1.75 – 1.69 (m, 1H), 1.39 (d, *J* = 7.0 Hz, 3H), 0.90 (t, *J* = 7.5 Hz, 3H), 0.89 (t, *J* = 7.0 Hz, 3H). ^{13}C NMR (125 MHz, $CDCl_3$, δ_C): 152.1, 137.4, 134.5, 133.9, 132.8, 131.2, 129.8, 126.8, 123.6, 118.5, 116.7, 115.2, 111.2, 73.7, 69.3, 67.1, 52.7, 50.7, 49.3, 30.7, 28.5, 19.3, 10.8, 7.7. HRMS (ESI) calcd for $C_{34}H_{39}Cl_2N_5O_4$: 652.2457; found 652.2426. HPLC Purity: 95.0%, tR = 13.4 min.

4-(4-(4-(4-(((*2S,4R*)-2-(bromomethyl)-2-(2,4-dichlorophenyl)-1,3-dioxolan-4-yl)methoxy)phenyl)piperazin-1-yl)phenyl)-1-*sec*-butyl-1*H*-1,2,4-triazol-5(4*H*)-one (10c). ^{1}H NMR (500 MHz, $CDCl_3$, δ_H): 7.65 (d, *J* = 8.5 Hz, 1H), 7.61 (s, 1H), 7.43-7.42 (m, 3H), 7.27 (dd, *J* = 8.5, 2.0 Hz, 1H), 7.03 (d, *J* = 9.0 Hz, 2H), 6.95 (bs, 2H), 6.90 (d, *J* = 9.0 Hz, 2H), 4.46-4.42 (m, 1H), 4.31-4.27 (m, 1H), 4.22 (dd, *J* = 9.5, 5.0 Hz, 1H), 4.14 (dd, *J* = 8.5, 5.5 Hz, 1H), 4.09 (dd, *J* = 8.5, 6.5 Hz, 1H), 4.02 (dd, *J* = 8.5, 7.0 Hz, 1H), 3.96 (d, *J* = 11.5, 1H), 3.86 (d, *J* = 11.5 Hz, 1H), 3.37 (bs, 4H), 3.25 (bs, 4H), 1.89 – 1.84 (m, 1H), 1.75 – 1.69 (m, 1H), 1.39 (d, *J* = 7.0 Hz, 3H), 0.90 (t, *J* = 7.5 Hz, 3H). ^{13}C NMR (125 MHz, $CDCl_3$, δ_C): 152.1, 135.7, 134.7, 133.9, 133.0, 131.3, 120.0, 127.0, 123.6, 118.5, 116.7, 115.5, 107.8, 74.8, 68.6, 68.4, 52.7, 50.7, 49.3, 35.4, 28.5, 19.3, 10.8. HRMS (ESI) calcd for $C_{33}H_{36}BrCl_2N_5O_4$: 716.1406; found 716.1422. HPLC Purity: 95.7%, tR = 13.3 min.

1-*sec*-butyl-4-(4-(4-(4-(((*2R,4R*)-2-(cyclopentylmethyl)-2-(2,4-dichlorophenyl)-1,3-dioxolan-4-yl)methoxy)phenyl)piperazin-1-yl)phenyl)-1*H*-1,2,4-triazol-5(4*H*)-one (10d).

^{1}H NMR (500 MHz, $CDCl_3$, δ_H): 7.62 (s, 1H), 7.58 (d, *J* = 8.0 Hz, 1H), 7.43 (d, *J* = 9.0 Hz, 2H), 7.39 (d, *J* = 2.5 Hz, 1H), 7.22 (dd, *J* = 8.5, 2.0 Hz, 1H), 7.03 (d, *J* = 9.0 Hz, 2H), 6.95 (bs, 2H), 6.89 (d, *J* = 9.0 Hz, 2H), 4.31-4.27 (m, 2H), 4.12 (dd, *J* = 9.2, 4.5 Hz, 1H), 3.99-3.95 (m, 2H), 3.84 (dd, *J* = 8.0, 7.0 Hz, 1H), 3.37 (bs, 4H), 3.24 (bs, 4H), 2.24– 2.16 (m, 2H), 1.90 – 1.81 (m, 2H), 1.75 – 1.69 (m, 3H),1.57 – 1.53 (m, 2H), 1.44 – 1.41 (m, 2H), 1.39 (d, *J* = 7.0 Hz, 3H), 1.14 – 1.06 (m, 2H), 0.90 (t, *J* = 7.5 Hz, 3H). ^{13}C NMR (125 MHz, $CDCl_3$, δ_C): 152.1, 137.8, 134.5, 133.9, 133.0, 131.2, 129.8, 126.6, 123.6, 118.5, 116.7, 115.5, 111.1, 73.6, 69.1, 66.8, 52.7, 50.7, 49.3, 43.6, 35.4, 33.6, 33.5, 28.5, 25.1, 25.0, 19.3, 10.8. HRMS (ESI) calcd for $C_{38}H_{45}Cl_2N_5O_4$: 706.2927; found 706.2915. HPLC Purity: 95.4%, tR = 15.2 min.

4-(4-(4-(4-(((*2R,4R*)-2-benzyl-2-(2,4-dichlorophenyl)-1,3-dioxolan-4-yl)methoxy)phenyl)piperazin-1-yl)phenyl)-1-*sec*-butyl-1*H*-1,2,4-triazol-5(4*H*)-one (10e). ^{1}H NMR (500 MHz, $CDCl_3$, δ_H): 7.62 (s, 1H), 7.46-7.42 (m, 4H), 7.43-7.42 (m, 3H), 7.22 (bs, 5H), 7.16 (dd, *J* = 8.5, 2.0 Hz, 1H), 7.03 (d, *J* = 9.0 Hz, 2H), 6.93 (bs, 2H), 6.73 (d, *J* = 9.0 Hz, 2H), 4.32-4.26 (m, 2H), 3.79-3.77 (m, 2H), 3.68 (dd, *J* = 9.5, 5.0 Hz, 1H), 3.45 (d, *J* = 14.0, 1H), 3.37 (bs, 4H), 3.34 (d, *J* = 14.0 Hz, 1H), 3.32-3.28 (m, 1H), 3.25 (bs, 4H), 1.89 – 1.84 (m, 1H), 1.75 – 1.69 (m, 1H), 1.39 (d, *J* = 6.5 Hz, 3H), 0.90 (t, *J* = 7.2 Hz, 3H). ^{13}C NMR (125 MHz, $CDCl_3$, δ_C): 152.1, 137.7, 135.2, 134.6, 133.9, 132.9, 131.3, 131.1, 129.5, 127.7, 123.6, 116.7, 115.3, 110.1, 74.0, 68.4, 67.2, 52.7, 49.2, 43.7, 36.5 28.5, 19.3, 10.8. HRMS (ESI) calcd for $C_{39}H_{41}Cl_2N_5O_4$: 714.2614; found 714.2590. HPLC Purity: 95.1%, tR = 14.8 min.

1-(sec-butyl)-4-(4-(4-(4-(((*2S,4R*)-2-(2,4-dichlorophenyl)-2-((dimethylamino)methyl)-1,3-dioxolan-4-yl)methoxy)phenyl)piperazin-1-yl)phenyl)-1*H*-1,2,4-triazol-5(4*H*)-one (11a). 1H NMR (500 MHz, CDCl3, δ_H): 8.41 (s, 1H), 7.74-7-75 (m, 2H), 7.59 (d, *J* = 9 Hz, 2H), 7.19 (d, *J* = 9 Hz, 2H), 7.06 (d, *J* = 9 Hz, 2H), 7.00 (d, *J* = 9 Hz, 2H), 4.53-4.48 (m, 1H), 4.23-4.18 (m, 3H), 4.10-4.03 (m, 4H), 3.43-3.38 (m, 4H), 3.27-3.24 (m, 4H), 2.59 (s, 6H), 1.84-1.78 (m, 1H), 1.76-1.70 (m, 1H), 1.38 (d, *J* = 6.5 Hz, 3H), 0.88 (t, *J* = 6.5 Hz, 3H). 13C NM R (125 MHz, CDCl3, δ_C): 152.8, 150.2, 146.5, 135.5, 134.2, 130.2, 127.0, 126.6, 124.3, 119.3, 117.5, 116.2, 77.2, 72.2, 68.4, 60.7, 50.4, 47.6, 29.9, 20.8, 12.4. HRMS (ESI) calcd for $C_{36}H_{40}Cl_2N_8O_4$: 681.2723; found 681.2714. HPLC Purity: 97.1%, tR = 4.7 min.

1-(sec-butyl)-4-(4-(4-(4-(((*2S,4R*)-2-(2,4-dichlorophenyl)-2-(morpholinomethyl)-1,3-dioxolan-4-yl)methoxy)phenyl)piperazin-1-yl)phenyl)-1*H*-1,2,4-triazol-5(4*H*)-one (11b).

^{1}H NMR (500 MHz, $CDCl_3$, δ_H): 7.63 (s, 1H), 7.61(d, J = 9.0 Hz, 1H), 7.45 (d, J = 8.5 Hz, 2H), 7.41(d, J = 1.5 Hz, 1H), 7.25(dd, J = 8, 1.5 Hz, 1H), 7.06(d, J = 9.0 Hz, 2H), 6.98(d, J = 9.0 Hz, 2H), 6.92(d, J = 8.5 Hz, 2H), 4.36-4.41 (m, 1H), 4.28-3.34 (m, 1H), 4.14-4.18 (m, 1H), 4.05-4.10 (m, 2H), 3.89 (t, J = 7.0 Hz, 1H), 3.57 (t, J = 4 Hz, 4H), 3.36-3.40 (m, 4H), 3.26 (t, J = 5 Hz, 4H), 2.59 (t, J = 4 Hz, 4H), 1.95-1.85 (m, 1H), 1.79-1.70 (m, 1H), 1.42 (d, J = 7 Hz, 3H), 0.93 (t, J = 7 Hz, 3H). ^{13}C NMR (125 MHz, $CDCl_3$, δ_C): 152.6, 151.1, 146.5, 135.3, 133.6, 131.6, 130.6, 127.2, 126.6, 124.3, 119.3, 117.5, 116.2, 75.2, 68.4, 56.0, 53.9, 51.9, 50.5, 31.1, 29.9, 20.8, 12.4. HRMS (ESI) calcd mass for $C_{37}H_{44}Cl_2N_6O_5$: 723.2828; found 723.2826. HPLC Purity: 96.2%, tR = 5.0 min.

1-(sec-butyl)-4-(4-(4-(4-(((*2S,4R*)-2-(2,4-dichlorophenyl)-2-(piperazin-1-ylmethyl)-1,3-dioxolan-4-yl)methoxy)phenyl)piperazin-1-yl)phenyl)-1*H*-1,2,4-triazol-5(4H)-one (11c). ^{1}H NMR (500 MHz, $CDCl_3$, δ_H): 7.62 (s, 1H), 7.60 (d, J = 8.5 Hz, 2H), 7.44 (d, J = 9 Hz, 2H), 7.39 (d, J = 1.5 Hz, 1H), 7.24 (dd, J = 8.5, 2.0 Hz, 1H), 7.04 (d, J = 8.5 Hz, 2H), 6.96 (d, J = 9 Hz, 2H), 6.90 (d, J = 9 Hz, 2H), 4.39-4.34 (m, 1H), 4.32-4.27 (m, 1H), 4.16-4.13 (m, 1H), 4.08-4.03 (m, 2H), 3.89 (t, J = 7.5 Hz, 1H), 3.56 (t, J = 4.5 Hz, 4H), 3.39-3.35 (m, 4H), 3.26-3.23 (m, 4H), 2.99 (d, J = 3 Hz, 3H), 2.57 (t, J = 4.5 Hz, 4H), 2.19 (s, 1H), 1.90-1.85 (m, 1H), 1.76-1.70 (m, 1H), 1.41 (d, J = 6.5 Hz, 3H), 0.92 (t, J = 7.5 Hz, 3H). ^{13}C NMR (125 MHz, $CDCl_3$, δ_C): 153.5, 151.1, 146.5, 137.4, 135.2, 133.6, 131.6, 130.6, 127.2, 126.6, 124.3, 119.3, 117.5, 116.2, 75.2, 70.0, 68.4, 68.2, 64.4, 56.0, 53.9, 51.9, 50.5, 29.9, 20.8, 12.4. HRMS (ESI) calcd for $C_{37}H_{45}Cl_2N_7O_4$: 722.7049; found 722.7043. HPLC Purity: 95.1%, tR = 5.1 min.

1-(sec-butyl)-4-(4-(4-(4-(((*2S,4R*)-2-(2,4-dichlorophenyl)-2-((4-methylpiperazin-1-yl)methyl)-1,3-dioxolan-4-yl)methoxy)phenyl)piperazin-1-yl)phenyl)-1*H*-1,2,4-triazol-5(4*H*)-one (11d). ^{1}H NMR (500 MHz, $CDCl_3$, δ_H): 8.03 (s, 1H), 7.62 (s, 1H), 7.58 (d, J = 8.5 Hz, 1H), 7.43 (d, J = 7.5 Hz, 2H), 7.38 (s, 1H), 7.23 (d, J = 8.5 Hz, 1H), 7.04 (d, J = 8 Hz, 2H), 6.96 (d, J = 8 Hz, 2H), 6.90 (d, J = 8 Hz, 2H), 4.36-4.34 (m, 1H), 4.32-4.28 (m, 1H), 4.15-4.12 (m, 1H), 4.06-4.02 (m, 2H), 3.87 (t, J = 7.5 Hz, 1H), 3.60-3.58 (m, 4H), 3.37-3.36 (m, 4H), 3.25-3.22 (m, 4H), 3.02 (s, 2H), 2.70-2.67 (m, 4H), 2.33 (s, 3H), 1.89-1.84 (m, 1H), 1.75-1.69 (m, 1H), 1.41 (d, J = 6.5 Hz, 3H), 0.91 (t, J = 7.5 Hz, 3H). ^{13}C NM R (125 MHz, $CDCl_3$, δ_C): 153.5, 152.6, 151.1, 146.5, 137.4, 135.2, 133.7, 131.6, 130.6, 127.2, 126.6, 124.3, 119.3, 117.5,

116.2, 75.2, 70.1, 68.2, 63.6, 55.8, 54.3, 53.9, 51.9, 50.5, 46.7, 29.9, 20.8, 12.4. HRMS (ESI) calcd for $C_{38}H_{47}Cl_2N_7O_4$: 736.7291; found 736.7252. HPLC Purity: 96.3%, tR = 7.5 min.

1-*sec*-butyl-4-(4-(4-(4-(((*2S,4R*)-2-(2,4-dichlorophenyl)-2-((3-methyl-1*H*-1,2,4-triazol-1-yl)methyl)-1,3-dioxolan-4-yl)methoxy)phenyl)piperazin-1-yl)phenyl)-1*H*-1,2,4-triazol-5(4*H*)-one (15a). ^{1}H NMR (500 MHz, $CDCl_3$, δ_H): 8.08 (bs, 1H), 7.62 (s, 1H), 7.60 (s, 1H), 7.46 (d, *J* = 2.0 Hz, 1H), 7.43 (d, *J* = 9.0 Hz, 2H), 7.26 (dd, *J* = 8.0, 2.0 Hz, 1H), 7.03 (d, *J* = 9.5 Hz, 2H), 6.98-6.97 (m, 2H), 6.80 (d, *J* = 9.0 Hz, 2H), 4.75 (d, *J* = 15.0 Hz, 1H), 4.65 (d, *J* = 15.0 Hz, 1H), 4.36 (dt, *J* = 6.5, 5.0, 2.5 Hz, 1H), 4.29 (dd, *J* = 8.5, 6.5 Hz, 1H), 3.90 (dd, *J* = 8.5, 6.5 Hz, 1H), 3.83 (dd, *J* = 8.5, 4.5 Hz, 1H), 3.77 (dd, *J* = 9.5, 5.0 Hz, 1H), 3.43 (dd, *J* = 9.5, 6.5 Hz, 1H), 3.39 (m, 4H), 3.25 (t, *J* = 5.0 Hz, 4H), 2.35 (s, 3H), 1.89 – 1.83 (m, 1H), 1.74 – 1.69 (m, 1H), 1.39 (d, *J* = 6.5 Hz, 3H), 0.90 (t, *J* = 7.5 Hz, 3H). ^{13}C NMR (125 MHz, $CDCl_3$, δ_C): 152.1, 145.3, 136.0, 134.3, 134.0, 133.2, 131.5, 129.7, 127.3, 123.7, 123.6, 118.7, 116.8, 115.3, 107.7, 74.7, 67.7, 67.5, 53.3, 52.7, 50.9, 49.2, 28.5, 19.3, 13.9, 10.8. HRMS (ESI) calcd for $C_{36}H_{40}Cl_2N_8O_4$: 719.2628; found 719.2614. HPLC Purity: 97.4%, tR = 9.2 min.

1-*sec*-butyl-4-(4-(4-(4-(((*2S,4R*)-2-(2,4-dichlorophenyl)-2-((3,5-dimethyl-1*H*-1,2,4-triazol-1-yl)methyl)-1,3-dioxolan-4-yl)methoxy)phenyl)piperazin-1-yl)phenyl)-1*H*-1,2,4-triazol-5(4*H*)-one (15b). ^{1}H NMR (500 MHz, $CDCl_3$, δ_H): 7.67 (d, *J* = 8.5 Hz, 1H), 7.61 (s, 1H), 7.47 (d, *J* = 2.0 Hz, 1H), 7.43 (d, *J* = 9.0 Hz, 2H), 7.29 (dd, *J* = 8.5, 2.0 Hz, 1H), 7.03 (d, *J* = 9.5 Hz, 2H), 6.97 (d, *J* = 9.5 Hz, 2H), 6.77 (dd, *J* = 7.0, 2.5 Hz, 2H), 4.64 (d, *J* = 15.0 Hz, 1H), 4.54 (d, *J* = 15.0 Hz, 1H), 4.36 (dt, *J* = 6.5, 5.0, 2.0 Hz, 1H), 4.29 (qt, *J* = 8.5, 6.5, 4.0 Hz, 1H), 3.84 (t, *J* = 5.0 Hz, 1H), 3.67 (dd, *J* = 5.0, 6.5 Hz, 1H), 3.39 (t, *J* = 5.0 Hz, 4H), 3.29-3.38 (m, 1H), 3.24 (t, *J* = 5.0 Hz, 4H), 2.51 (s, 3H), 2.30 (s, 3H), 1.89 – 1.83 (m, 1H), 1.74 – 1.69 (m, 1H), 1.39 (d, *J* = 6.5 Hz, 3H), 0.90 (t, *J* = 7.5 Hz, 3H). ^{13}C NMR (125 MHz, $CDCl_3$, δ_C): 159.0, 154.5, 152.1, 150.5, 136.0, 134.7, 134.0, 133.1, 131.4, 129.8, 127.3, 127.1, 126.0, 123.6, 123.6, 118.7, 116.8, 116.2, 115.2, 108.6, 74.6, 67.6, 67.3, 52.7, 51.9, 50.8, 49.2, 28.5, 19.3, 13.7, 10.8. HRMS (ESI) calcd for $C_{37}H_{42}Cl_2N_8O_4$: 733.2784; found 733.2764. HPLC Purity: 95.4%, tR = 7.9 min.

1-*sec*-butyl-4-(4-(4-(4-(((*2S,4R*)-2-(2,4-dichlorophenyl)-2-((3-(trifluoromethyl)-1*H*-1,2,4-triazol-1-yl)methyl)-1,3-dioxolan-4-yl)methoxy)phenyl)piperazin-1-yl)phenyl)-1*H*-1,2,4-triazol-5(4*H*)-one (15c). ^{1}H NMR (500 MHz, $CDCl_3$, δ_H): 8.32 (s, 1H), 7.62 (bs, 1H), 7.60 (s,

1H), 7.49 (d, *J* = 2.0 Hz, 1H), 7.43 (d, *J* = 8.5 Hz, 2H), 7.29 (dd, *J* = 8.5, 2.0 Hz, 1H), 7.03 (d, *J* = 9.0 Hz, 2H), 6.94-6.91 (m, 2H), 6.79 (d, *J* = 8.0 Hz, 2H), 4.87 (d, *J* = 15.0 Hz, 1H), 4.80 (d, *J* = 15.0 Hz, 1H), 4.37 (t, *J* = 5.0 Hz, 1H), 4.29 (dd, *J* = 8.5, 6.5, 2.0 Hz, 1H), 3.93 (dd, *J* = 8.5, 7.0 Hz, 1H), 3.82 (dd, *J* = 8.5, 5.0 Hz, 1H), 3.80 (dd, *J* = 10.0, 4.5 Hz, 1H), 3.49 (dd, *J* = 9.5, 6.0 Hz, 1H), 3.37 (bs, 4H), 3.25 (bs, 4H), 1.89 – 1.83 (m, 1H), 1.74 – 1.69 (m, 1H), 1.39 (d, *J* = 7.0 Hz, 3H), 0.90 (t, *J* = 7.5 Hz, 3H). ^{13}C NMR (125 MHz, $CDCl_3$, δ_C): 162.6, 152.1, 146.6, 136.3, 134.0, 133.6, 133.2, 131.5, 129.7, 127.4, 123.6, 116.7, 115.2, 107.2, 74.7, 67.4, 67.4, 54.1, 52.7, 49.2, 36.5, 28.5, 19.3, 10.8. HRMS (ESI) calcd for $C_{36}H_{37}Cl_2F_3N_8O_4$: 773.2345; found 773.2357. HPLC Purity: 95.5%, tR = 12.2 min.

4-(4-(4-(4-(((*2S,4R*)-2-((1*H*-imidazol-1-yl)methyl)-2-(2,4-dichlorophenyl)-1,3-dioxolan-4-yl)methoxy)phenyl)piperazin-1-yl)phenyl)-1-*sec*-butyl-1*H*-1,2,4-triazol-5(4*H*)-one (15d). ^{1}H NMR (500 MHz, $CDCl_3$, δ_H): 7.61 (s, 1H), 7.58 (d, *J* = 8.0 Hz, 1H), 7.53 (bs, 1H), 7.46 (d, *J* = 2.5 Hz, 1H), 7.42 (d, *J* = 9.5 Hz, 2H), 7.26 (dd, *J* = 8.2, 2.2 Hz, 2H), 7.03 (d, *J* = 9 Hz, 2H), 7.00-6.98 (m, 1H), 6.93 (d, *J* = 9.0 Hz, 2H), 6.78 (d, *J* = 9.5 Hz, 2H), 4.51 (d, *J* = 15.0 Hz, 1H), 4.41 (d, *J* = 15.0 Hz, 1H), 4.41 (d, *J* = 15.0 Hz, 1H), 4.34 – 4.28 (m, 2H), 3.87 (dd, *J* = 8.5, 6.5 Hz, 1H), 3.74 – 3.72 (m, 2H), 3.36 (t, *J* = 5.0 Hz, 4H), 3.32 – 3.31 (m, 1H), 3.23 (t, *J* = 5.0 Hz, 4H), 1.89 – 1.83 (m, 1H), 1.74 – 1.71 (m, 1H), 1.39 (d, *J* = 7.0 Hz, 3H), 0.90 (t, *J* = 7.0 Hz, 3H). ^{13}C NMR (125 MHz, $CDCl_3$, δ_C): 152.7, 152.1, 150.6, 146.0, 136.0, 134.6, 134.0, 133.0, 131.4, 129.5, 127.3, 125.9, 123.6, 118.5, 116.7, 115.3, 108.0, 74.8, 67.7, 67.6, 52.7, 50.6, 49.3, 28.5, 19.3, 10.8. HRMS (ESI) calcd for $C_{36}H_{39}Cl_2N_7O_4$: 704.2519; found 704.2525. HPLC Purity: 95.3%, tR = 8.3 min.

1-*sec*-butyl-4-(4-(4-(4-(((*2S,4R*)-2-(2,4-dichlorophenyl)-2-((2-methyl-1*H*-imidazol-1-yl)methyl)-1,3-dioxolan-4-yl)methoxy)phenyl)piperazin-1-yl)phenyl)-1*H*-1,2,4-triazol-5(4*H*)-one (15e). ^{1}H NMR (500 MHz, $CDCl_3$, δ_H): 7.63 (d, *J* = 8.5 Hz, 1H), 7.61 (s, 1H), 7.47 (d, *J* = 2.0 Hz, 1H), 7.42 (d, *J* = 9.0 Hz, 2H), 7.29 (dd, *J* = 8.5, 2.0 Hz, 1H), 7.03 (d, *J* = 9.0 Hz, 2H), 6.94-6.90 (m, 3H), 6.77 (d, *J* = 9.5 Hz, 2H), 4.41 (d, *J* = 15.0 Hz, 1H), 4.34 (d, *J* = 15.0 Hz, 1H), 4.32 – 4.26 (m, 2H), 3.85 (dd, *J* = 8.5, 6.5 Hz, 1H), 3.76-3.73 (m, 1H), 3.66 (dd, *J* = 9.5, 5.0 Hz, 1H), 3.36 (t, *J* = 4.5 Hz, 4H), 3.24-3.22 (m, 5H), 2.49 (s, 3H), 1.89 – 1.84 (m, 1H), 1.74 – 1.69 (m, 1H), 1.39 (d, *J* = 6.5 Hz, 3H), 0.90 (t, *J* = 7.5 Hz, 3H). ^{13}C NMR (125 MHz, $CDCl_3$, δ_C): 152.7, 152.1, 150.6, 146.0, 136.0, 134.0, 133.1, 131.6, 129.6, 127.3, 125.9,

123.6, 118.5, 116.7, 115.3, 108.6, 74.8, 67.6, 67.4, 52.7, 50.6, 49.3, 43.2, 28.5, 19.3, 10.8. HRMS (ESI) calcd for $C_{37}H_{41}Cl_2N_7O_4$: 718.2675; found 718.2645. HPLC Purity: 95.0%, tR = 5.3 min

1-(sec-butyl)-4-(4-(4-(4-(((*2S,4R*)-2-(2,4-dichlorophenyl)-2-((2-ethyl-1*H*-imidazol-1-yl)methyl)-1,3-dioxolan-4-yl)methoxy)phenyl)piperazin-1-yl)phenyl)-1*H*-1,2,4-triazol-5(4*H*)-one (15f).

7.65 (d, *J* = 8.5 Hz, 1H), 7.62 (s, 1H), 7.48 (d, *J* = 2 Hz, 1H), 7.43 (d, *J* = 9.0 Hz, 2H), 7.30 (dd, *J* = 8.5, 2.0 Hz, 1H), 7.04 (d, *J* = 9 Hz, 2H), 6.95-6.92 (m, 4H), 6.77 (d, *J* = 9.0 Hz, 2H), 4.51 (d, *J* = 15.0 Hz, 1H), 4.44 (d, *J* = 15.0 Hz, 1H), 4.38 (d, *J* = 15.0 Hz, 1H), 4.35 – 4.27 (m, 2H), 3.86 (dd, *J* = 8.5, 6.5 Hz, 1H), 3.76 (dd, *J* = 8.5, 4.5 Hz, 1H), 3.65 (dd, *J* = 9.5, 5.2 Hz, 1H), 3.37 (t, *J* = 5.0 Hz, 4H), 3.24 (t, *J* = 5.0 Hz, 4H), 3.15 (t, *J* = 8.5 Hz, 1H), 2.8(q, *J* = 7.5 Hz, 2H), 1.90 – 1.84 (m, 1H), 1.75 – 1.70 (m, 1H), 1.41 (d, *J* = 6.5 Hz, 3H), 1.34 (3t, *J* = 7.5 Hz, 3H), 0.91 (t, *J* = 7.5 Hz, 3H). ^{13}C NMR (125 MHz, $CDCl_3$, δ_C): 153.2, 152.6, 151.3, 151.1, 146.4, 136.5, 135.7, 133.8, 132.1, 130.2, 128.0, 127.2, 126.6, 124.3, 122.3, 119.2, 117.4, 116.0, 109.5, 75.9, 68.7, 68.6, 53.9, 51.9, 50.8, 50.5, 29.9, 21.5, 20.8, 13.4, 12.4. HRMS (ESI) calcd for $C_{38}H_{43}Cl_2N_7O_4$: 732.2832; found 732.2855. HPLC Purity: 98.2%, tR = 5.6 min.

1-*sec*-butyl-4-(4-(4-(4-(((*2S,4R*)-2-(2,4-dichlorophenyl)-2-((2-isopropyl-1*H*-imidazol-1-yl)methyl)-1,3-dioxolan-4-yl)methoxy)phenyl)piperazin-1-yl)phenyl)-1*H*-1,2,4-triazol-5(4*H*)-one (15g). ^{1}H NMR (500 MHz, $CDCl_3$, δ_H): 7.63 (d, *J* = 8.5 Hz, 1H), 7.61 (s, 1H), 7.48 (d, *J* = 2.5 Hz, 1H), 7.42 (d, *J* = 9.0 Hz, 2H), 7.29 (dd, *J* = 8.5, 2.0 Hz, 1H), 7.03 (d, *J* = 9 Hz, 2H), 6.97 (bs, 1H), 6.94 (s, 1H), 6.93-6.92 (m, 2H), 6.75 (d, *J* = 9.0 Hz, 2H), 4.51 (d, *J* = 15.0 Hz, 1H), 4.44 (d, *J* = 15.0 Hz, 1H), 4.38 (d, *J* = 15.0 Hz, 1H), 4.35 – 4.27 (m, 2H), 3.85 (dd, *J* = 8.5, 6.5 Hz, 1H), 3.76 (dd, *J* = 8.5, 4.5 Hz, 1H), 3.66 (dd, *J* = 9.5, 5.2 Hz, 1H), 3.36 (t, *J* = 5.2 Hz, 4H), 3.26 (t, *J* = 7.0 Hz, 1H), 3.23 (t, *J* = 5.0 Hz, 4H), 1.89 – 1.83 (m, 1H), 1.74 – 1.69 (m, 1H), 1.39 (d, *J* = 6.5 Hz, 3H), 1.34 (d, *J* = 7.0 Hz, 3H), 1.31 (d, *J* = 6.5 Hz, 3H), 0.90 (t, *J* = 7.5 Hz, 3H). ^{13}C NMR (125 MHz, $CDCl_3$, δ_C): 154.4, 152.6, 152.0, 150.6, 146.0, 136.0, 133.9, 133.1, 131.5, 129.6, 127.4, 125.9, 123.6, 121.3, 118.5, 116.7, 115.2, 108.3, 74.8, 67.6, 67.6, 52.7, 50.6, 49.3, 28.5, 25.5, 22.0, 21.6, 19.3, 10.8. HRMS (ESI) calcd for $C_{39}H_{45}Cl_2N_7O_4$: 746.2988; found 746.2996. HPLC Purity: 95.8%, tR = 6.0 min.

1-*sec*-butyl-4-(4-(4-(4-(((*2S,4R*)-2-(2,4-dichlorophenyl)-2-((2-phenyl-1*H*-imidazol-1-yl)methyl)-1,3-dioxolan-4-yl)methoxy)phenyl)piperazin-1-yl)phenyl)-1*H*-1,2,4-triazol-5(4*H*)-one (15h). ^{1}H NMR (500 MHz, $CDCl_3$, δ_H): 7.61 (s, 2H), 7.60 (d, *J* = 3.5 Hz, 1H), 7.51 (d, *J* = 8.5 Hz, 1H), 7.43-7.40 (m, 5H), 7.30 (d, *J* = 2.5 Hz, 1H), 7.25 (d, *J* = 1.5 Hz, 1H), 7.22 (dd, *J* = 8.5, 2.5 Hz, 1H), 7.13 (s, 1H), 7.03 (d, *J* = 9.5 Hz, 2H), 6.94 (d, *J* = 9.5 Hz, 2H), 6.79 (d, *J* = 9.5 Hz, 2H), 4.56 (s, 2H), 4.38 – 4.27 (m, 2H), 3.89-3.87 (m, 2H), 3.80 (dd, *J* = 9.5, 5.0 Hz, 1H), 3.50 (dd, *J* = 9.5, 6.5 Hz, 1H), 3.37-3.34 (m, 5H), 3.23 (t, *J* = 5.5 Hz, 4H), 3.20-3.19 (m, 1H), 1.88 – 1.83 (m, 1H), 1.74 – 1.70 (m, 1H), 1.39 (d, *J* = 6.5 Hz, 3H), 0.90 (t, *J* = 7.5 Hz, 3H). ^{13}C NMR (125 MHz, $CDCl_3$, δ_C):152.6, 152.0, 150.6, 146.0, 133.9, 131.4, 129.6, 129.5, 128.5, 127.1, 125.9, 123.6, 123.0, 118.9, 116.0, 115.3, 108.4, 74.7, 67.9, 67.3, 52.7, 50.6, 49.3, 28.5, 19.3, 10.8. HRMS (ESI) calcd for $C_{42}H_{43}Cl_2N_7O_4$: 780.2832; found 780.2819. HPLC Purity: 95.6%, tR = 6.5 min.

1-*sec*-butyl-4-(4-(4-(4-(((*2S,4R*)-2-(2,4-dichlorophenyl)-2-((4-methyl-1*H*-imidazol-1-yl)methyl)-1,3-dioxolan-4-yl)methoxy)phenyl)piperazin-1-yl)phenyl)-1*H*-1,2,4-triazol-5(4*H*)-one (15i). ^{1}H NMR (500 MHz, $CDCl_3$, δ_H): 7.61 (s, 1H), 7.58 (d, *J* = 8.5 Hz, 1H), 7.49 (bs, 1H), 7.46 (d, *J* = 2.0 Hz, 1H), 7.42 (d, *J* = 9.0 Hz, 2H), 7.27-7.25 (m, 1H), 7.03 (d, *J* = 9.0 Hz, 2H), 6.94 (dd, *J* = 9.0, 2.0 Hz, 2H), 6.78 (d, *J* = 9.0 Hz, 2H), 6.69 (bs, 1H), 4.43 (d, *J* = 15.0 Hz, 1H), 4.34 (d, *J* = 15.0 Hz, 1H), 4.33 – 4.27 (m, 2H), 3.86 (dd, *J* = 8.5, 6.5 Hz, 1H), 3.79 (dd, *J* = 8.5, 4.5 Hz, 1H), 3.71 (dd, *J* = 9.5, 5.0 Hz, 1H), 3.36 (t, *J* = 4.5 Hz, 4H), 3.29 (dd, *J* = 9.5, 6.5 Hz, 1H), 3.23 (t, *J* = 5.0 Hz, 4H), 2.18 (s, 3H), 1.89 – 1.83 (m, 1H), 1.74 – 1.69 (m, 1H), 1.39 (d, *J* = 6.5 Hz, 3H), 0.90 (t, *J* = 7.5 Hz, 3H). ^{13}C NMR (125 MHz, $CDCl_3$, δ_C): 152.7, 152.1, 150.6, 146.0, 136.0, 134.6, 134.0, 133.0, 131.4, 129.6, 127.3, 125.9, 123.6, 118.5, 116.7, 115.2, 108.0, 74.8, 67.7, 67.5, 52.7, 51.4, 50.7, 49.3, 28.5, 19.3, 10.8. HRMS (ESI) calcd for $C_{37}H_{41}Cl_2N_7O_4$: 718.2675; found 718.2697. HPLC Purity: 95.7%, tR = 5.3 min.

1-(sec-butyl)-4-(4-(4-(4-(((*2S,4R*)-2-(2,4-dichlorophenyl)-2-((2,4-dimethyl-1*H*-imidazol-1-yl)methyl)-1,3-dioxolan-4-yl)methoxy)phenyl)piperazin-1-yl)phenyl)-1*H*-1,2,4-triazol-5(4*H*)-one (15j). ^{1}H NMR (500 MHz, $CDCl_3$, δ_H): 7.65 (d, *J* = 8.5 Hz, 1H), 7.61 (s, 1H), 7.43-7.40 (m, 3H), 7.24 (s, 1H), 7.03 (d, *J* = 8.5 Hz, 2H), 6.89 (d, *J* = 8.5 Hz, 2H), 6.73 (s, 1H), 6.66 (d, *J* = 8.5 Hz, 2H), 4.35-4.24 (m, 3H), 4.18-4.15 (m, 1H), 3.94 (t, *J* = 7.5 Hz, 1H), 3.89-3.86 (m, 1H), 3.82-3.79 (m, 1H), 3.75 (t, *J* = 7.5 Hz, 1H), 3.33-3.37 (m, 4H), 3.20-3.22 (m, 4H),

2.50 (s, 3H), 2.20 (s, 3H), 1.90-1.82 (m, 1H), 1.75-1.70 (m, 1H), 1.40 (d, J = 6.5 Hz, 3H), 0.91 (t, J = 7.5 Hz, 3H). ^{13}C NMR (125 MHz, $CDCl_3$, δ_C): 152.6,152.0, 150.2, 146.9, 136.2, 143.0, 134.1, 133.8, 131.2, 129.6, 127.2, 125.5, 122.5, 118.2, 117.5, 115.2, 108.2, 75.3, 67.9, 67.4, 52.5, 50.7, 49.4, 28.7, 15.6, 14.2, 10.8. HRMS (ESI) calcd for $C_{38}H_{43}Cl_2N_7O_4$: 732.2832; found 732.2803. HPLC Purity: 94.8%, tR = 5.0 min

1-(sec-butyl)-4-(4-(4-(4-(((*2S,4R*)-2-(2,4-dichlorophenyl)-2-((2,5-dimethyl-1*H*-imidazol-1-yl)methyl)-1,3-dioxolan-4-yl)methoxy)phenyl)piperazin-1-yl)phenyl)-1*H*-1,2,4-triazol-5(4*H*)-one (15k). ^{1}H NMR (500 MHz, $CDCl_3$, δ_H): 7.73 (d, J = 8.5 Hz, 1H), 7.61 (s, 1H), 7.45-7.41 (m, 3H), 7.24 (s, 1H), 7.03 (d, J = 8.5 Hz, 2H), 6.89 (d, J = 8.5 Hz, 2H), 6.67-6.65 (m, 3H), 4.33-4.27 (m, 2H), 4.24-4.21 (m, 1H), 4.02-3.98 (m, 1H), 3.85-3.84 (d, J = 4.5 Hz, 1H), 3.81-3.76 (m, 2H), 3.72 (t, J = 1.5 Hz, 1H), 3.37-3.34 (m, 4H), 3.24-3.20 (m, 4H), 2.51 (s, 3H), 2.30 (s, 3H), 1.90-1.85 (m, 1H), 1.75-1.70 (m, 1H), 1.41 (d, J = 6.5 Hz, 3H), 0.93 (t, J = 7.5 Hz, 3H). ^{13}C NMR (125 MHz, $CDCl_3$, δ_C): 152.7,152.0, 150.2, 146.9, 136.2, 142.7, 134.1, 133.8, 131.2, 128.0, 127.2, 125.5, 122.0, 118.2, 117.5, 115.2, 108.2, 75.3, 67.9, 67.4, 52.5, 50.7 49.7, 28.7, 14.0, 10.8. HRMS (ESI) calcd for $C_{38}H_{43}Cl_2N_7O_4$: 732.2832; found 732.2837. HPLC Purity: 95.0%, tR = 5.2 min.

1-(sec-butyl)-4-(4-(4-(4-(((*2S,4R*)-2-(2,4-dichlorophenyl)-2-((2-methyl-4-(trifluoromethyl)-1*H*-imidazol-1-yl)methyl)-1,3-dioxolan-4-yl)methoxy)phenyl)piperazin-1-yl)phenyl)-1*H*-1,2,4-triazol-5(4*H*)-one (15l). ^{1}H NMR (500 MHz, $CDCl_3$, δ_H): 7.64 (d, J = 8.5 Hz, 2H), 7.61 (s, 1H), 7.48 (d, J = 1.5 Hz, 1H), 7.42 (d, J = 9 Hz, 2H), 7.31-7.29 (m, 2H), 7.03 (d, J = 9 Hz, 2H), 6.93 (d, J = 9 Hz, 2H), 6.75 (d, J = 9 Hz, 2H), 4.44-4.41 (m, 1H), 4.37-4.26 (m, 3H), 3.85 (t, J = 8.5 Hz, 1H), 3.78-3.76 (m, 1H), 3.65 (q, J = 4.5 Hz, 1H), 3.32-3.38 (m, 4H), 3.40-3.20 (m, 4H), 2.48 (s, 3H), 1.90-1.84 (m, 1H), 1.75-1.69 (m, 1H), 1.40 (d, J = 6.5 Hz, 3H), 0.91 (t, J = 7.5 Hz, 3H). ^{13}C NMR (125 MHz, $CDCl_3$, δ_C): 152.7, 152.1, 150.6, 146.0, 136.1, 134.5, 133.0, 132.0, 129.6, 127.2, 125.9, 123.6, 121.9, 118.6, 116.5, 107.2, 74.7, 67.8, 52.7, 50.8, 49.3, 28.5, 19.3, 14.1, 10.8. HRMS (ESI) calcd for $C_{38}H_{40}Cl_2F_3N_7O_4$: 786.2549; found 786.2562. HPLC Purity: 95.7%, tR = 11.9 min.

4-(4-(4-(4-(((*2S,4R*)-2-((1*H*-pyrazol-1-yl)methyl)-2-(2,4-dichlorophenyl)-1,3-dioxolan-4-yl)methoxy)phenyl)piperazin-1-yl)phenyl)-1-*sec*-butyl-1*H*-1,2,4-triazol-5(4*H*)-one (15m). ^{1}H NMR (500 MHz, $CDCl_3$, δ_H): 7.62 (s, 1H), 7.58 (d, J = 8.5 Hz, 1H), 7.49 (t, J = 2.2 Hz,

2H), 7.45 (d, *J* = 2.0 Hz, 1H), 7.43 (d, *J* = 9.0 Hz, 2H), 7.22 (dd, *J* = 9.5, 2.0 Hz, 1H), 7.03 (d, *J* = 9.5 Hz, 2H), 6.93 (d, *J* = 8.5 Hz, 2H), 6.77 (d, *J* = 9.0 Hz, 2H), 6.22 (t, *J* = 2.0 Hz, 1H), 4.79 (d, *J* = 14.5 Hz, 1H), 4.68 (d, *J* = 15.0 Hz, 1H), 4.36-4.33 (m, 1H), 4.31-4.27 (m, 1H), 3.87 (dd, *J* = 8.5, 6.5 Hz, 1H), 3.80 (dd, *J* = 8.5, 4.5 Hz, 1H), 3.77 (dd, *J* = 8.5, 5.0 Hz, 1H), 3.37-3.31 (m, 5H), 3.24 (bs, 4H), 1.90 – 1.84 (m, 1H), 1.74 – 1.70 (m, 1H), 1.39 (d, *J* = 6.5 Hz, 3H), 0.90 (t, *J* = 7.2 Hz, 3H). ^{13}C NMR (125 MHz, $CDCl_3$, δ_C): 152.1, 139.4, 135.6, 135.0, 134.0, 133.2, 133.3, 131.2, 129.7, 127.1, 123.6, 118.5, 116.7, 115.3, 108.5, 105.8, 74.6, 68.0, 67.6, 56.1, 52.7, 50.7, 49.3, 28.5, 19.3, 10.8. HRMS (ESI) calcd for $C_{36}H_{39}Cl_2N_7O_4$: 704.2519; found 704.2542. HPLC Purity: 95.9%, tR = 11.6 min.

4-(4-(4-(4-(((*2S,4R*)-2-((1*H*-tetrazol-1-yl)methyl)-2-(2,4-dichlorophenyl)-1,3-dioxolan-4-yl)methoxy)phenyl)piperazin-1-yl)phenyl)-1-*sec*-butyl-1*H*-1,2,4-triazol-5(4*H*)-one (15n). ^{1}H NMR (500 MHz, $CDCl_3$, δ_H): 8.46 (s, 1H), 7.61 (s, 1H), 7.55 (d, *J* = 8.5 Hz, 1H), 7.48 (d, *J* = 2.0 Hz, 1H), 7.43 (d, *J* = 9 Hz, 2H), 7.24 (dd, *J* = 8.5, 2.0 Hz, 1H), 7.03 (d, *J* = 9.0 Hz, 2H), 6.81 (d, *J* = 9.0 Hz, 2H), 5.36 (d, *J* = 14.0 Hz, 1H), 5.27 (d, *J* = 14.0 Hz, 1H), 4.38 (t, *J* = 5.0 Hz, 1H), 4.31-4.27 (m, 1H), 3.95 (dd, *J* = 8.5, 6.5 Hz, 1H), 3.88 – 3.83 (m, 2H), 3.53 (dd, *J* = 9.5, 6.5 Hz, 1H), 3.38 (bs, 4H), 3.26 (bs, 4H), 1.89 – 1.83 (m, 1H), 1.74 – 1.69 (m, 1H), 1.39 (d, *J* = 7.0 Hz, 3H), 0.90 (t, *J* = 7.5 Hz, 3H). ^{13}C NMR (125 MHz, $CDCl_3$, δ_C): 162.5, 152.8, 152.7, 152.0, 136.3, 133.9, 133.3, 131.5, 130.1, 129.6, 127.2, 123.6, 116.8, 115.4, 107.4, 74.8, 67.9, 67.6, 56.6, 52.7, 36.5, 31.0, 28.5, 19.2, 10.8. HRMS (ESI) calcd for $C_{34}H_{37}Cl_2N_9O_4$: 706.2424; found 706.2425. HPLC Purity: 95.9%, tR = 10.5 min.

4-(4-(4-(4-(((*2S,4R*)-2-((2*H*-tetrazol-2-yl)methyl)-2-(2,4-dichlorophenyl)-1,3-dioxolan-4-yl)methoxy)phenyl)piperazin-1-yl)phenyl)-1-*sec*-butyl-1*H*-1,2,4-triazol-5(4*H*)-one (15o). ^{1}H NMR (500 MHz, $CDCl_3$, δ_H): 8.79 (s, 1H), 7.99 (s, 1H), 7.61 (s, 1H), 7.58 (d, *J* = 8.5 Hz, 1H), 7.48 (d, *J* = 2.0 Hz, 1H), 7.42-7.40 (m, 2H), 7.28-7.26 (m, 1H), 7.01 (d, *J* = 9.0 Hz, 2H), 6.79 (d, *J* = 9.0 Hz, 2H), 5.03 (d, *J* = 4.0 Hz, 2H), 4.34 (t, *J* = 9.0 Hz, 1H), 4.29-4.25 (m, 1H), 3.91 (dd, *J* = 8.5, 7.0 Hz, 1H), 3.77 – 3.74 (m, 2H), 3.56 (dd, *J* = 10.0, 5.5 Hz, 1H), 3.35 (bs, 4H), 3.23 (d, *J* = 5.0 Hz, 4H), 1.88 – 1.82 (m, 1H), 1.73 – 1.67 (m, 1H), 1.37 (d, *J* = 7.0 Hz, 3H), 0.88 (t, *J* = 7.5 Hz, 3H). ^{13}C NMR (125 MHz, $CDCl_3$, δ_C): 162.9, 151.9, 151.7, 151.5, 136.3, 133.9, 133.9, 131.5, 131.0, 129.6, 126.9, 123.4, 116.6, 115.4, 107.4, 74.8, 67.9, 67.6,

56.6, 52.7, 36.5, 31.2, 28.5, 19.2, 10.7. HRMS (ESI) calcd for $C_{34}H_{37}Cl_2N_9O_4$: 706.2424; found 706.2425. HPLC Purity: 94.6%, tR = 10.4 min.

1-*sec*-butyl-4-(4-(4-(4-(((*2S,4R*)-2-(2,4-dichlorophenyl)-2-((5-methyl-1*H*-tetrazol-1-yl)methyl)-1,3-dioxolan-4-yl)methoxy)phenyl)piperazin-1-yl)phenyl)-1*H*-1,2,4-triazol-5(4*H*)-one (15p). ^{1}H NMR (500 MHz, $CDCl_3$, δ_H): 7.61 (s, 1H), 7.59 (d, *J* = 8.5 Hz, 1H), 7.48 (d, *J* = 2.0 Hz, 1H), 7.43 (d, *J* = 9 Hz, 2H), 7.26 (dd, *J* = 8.0, 2.5 Hz, 1H), 7.03 (d, *J* = 9.0 Hz, 2H), 6.80 (d, *J* = 8.5 Hz, 2H), 5.27 (d, *J* = 14.5 Hz, 1H), 5.15 (d, *J* = 14.5 Hz, 1H), 4.39 (dt, *J* = 6.5, 5.0, 1.5 Hz, 1H), 4.31-4.27 (m, 1H), 3.95-3.87 (m, 2H), 3.80 (dd, *J* = 9.5, 4.7 Hz, 1H), 3.76 (dd, *J* = 9.0, 7.0 Hz, 1H), 3.38 (bs, 4H), 3.27 (bs, 4H), 2.47 (s, 3H), 1.89 – 1.83 (m, 1H), 1.74 – 1.69 (m, 1H), 1.39 (d, *J* = 7.0 Hz, 3H), 0.90 (t, *J* = 7.5 Hz, 3H). ^{13}C NMR (125 MHz, $CDCl_3$, δ_C): 171.2, 162.9, 152.1, 133.9, 133.5, 131.5, 129.6, 127.2, 123.6, 117.7, 115.4, 107.5, 74.7, 67.9, 67.5, 60.4, 56.4, 52.7, 28.5, 21.1, 19.3, 14.2, 10.8. HRMS (ESI) calcd for $C_{35}H_{39}Cl_2N_9O_4$: 720.2580; found 720.2571. HPLC Purity: 94.8%, tR = 11.3 min.

1-*sec*-butyl-4-(4-(4-(4-(((*2S,4R*)-2-(2,4-dichlorophenyl)-2-((5-phenyl-1*H*-tetrazol-1-yl)methyl)-1,3-dioxolan-4-yl)methoxy)phenyl)piperazin-1-yl)phenyl)-1*H*-1,2,4-triazol-5(4*H*)-one (15q). ^{1}H NMR (500 MHz, $CDCl_3$, δ_H): 8.15-8.13 (m, 2H), 8.02 (bs, 1H), 7.63-7.59 (m, 2H), 7.50 (d, *J* = 2.5 Hz, 1H), 7.48-7.46 (m, 2H), 7.44-7.41 (m, 2H), 7.26 (dd, *J* = 8.5, 2.0 Hz, 1H), 7.03 (d, *J* = 9.0 Hz, 2H), 6.67 (d, *J* = 9.0 Hz, 2H), 5.35 (d, *J* = 14.5 Hz, 1H), 5.24 (d, *J* = 14.5 Hz, 1H), 4.41-4.34 (m, 1H), 4.29 (dd, *J* = 9.0, 6.5 Hz, 1H), 3.94 (dd, *J* = 9.0, 6.5 Hz, 1H), 3.88 (dd, *J* = 8.5, 4.5 Hz, 1H), 3.81 (dd, *J* = 9.5, 4.5 Hz, 1H), 3.44 (dd, *J* = 9.5, 6.5 Hz, 1H), 3.35 (bs, 4H), 3.20 (bs, 4H), 1.89 – 1.83 (m, 1H), 1.75 – 1.69 (m, 1H), 1.39 (d, *J* = 6.5 Hz, 3H), 0.90 (t, *J* = 7.5 Hz, 3H). ^{13}C NMR (125 MHz, $CDCl_3$, δ_C): 196.5, 133.9, 133.4, 131.5, 129.7, 128.9, 127.0, 123.6, 118.4, 115.3, 107.5, 57.4, 56.7, 52.7, 32.2, 28.5, 19.3, 10.8. HRMS (ESI) calcd for $C_{40}H_{41}Cl_2N_9O_4$: 782.2737; found 782.2749. HPLC Purity: 95.7%, tR = 13.7 min.

HUVEC Culture and Proliferation Assays

HUVEC (Lonza) were grown in EGM-2 bullet kit media (Lonza) and used at passage eight or lower. The [^{3}H] thymidine incorporation assay was conducted as previously described.[32] Briefly, cells were seeded in 96-well plates at a concentration of 2000 cells/well and allowed

to settle overnight. Drugs were added to each well in triplicate. After 24 h, cells were treated with 1 μCi of [^{3}H] thymidine for 6 h. Then cells were harvested and transferred to filter mats, scintillation counted and IC_{50} were calculated using Graph Pad Prism software (version 6.0)

CYP3A4 enzyme assay

Inhibition of CYP3A4 enzyme activity was tested using Vivid™ CYP3A4 Green Screening Kit (ThermoFisher, #P2857) according to the manufacturer`s protocol. Briefly, CYP3A4 baculosomes and drugs were incubated at 37℃ for 10 min. Then Vivid® Substrates were added and the fluorescence (ex/em:485/520) were read 60 min after substrate added. The percent inhibition was calculated using 10 μM ketoconazole as 100% inhibition control.

Tube formation assay

Twenty four-well plates were coated with 250 μl matrigel (BD, #CB-40234C) per well. HUVEC (70,000) were added to the plate with 500 μL media with different drugs. After 24 h, 2 μM calcein AM was added and incubated for 15 min. After replacing with new media, the tube network was photographed using fluorescent microscopy. The total tube length was calculated using ImageJ and plotted using GraphPad Prism.

Filipin staining

HUVEC (2,000) were plated in chamber slide with 1ml media and allowed to settle overnight. Cells were treated with 0.1 μM drug or DMSO for 14 h. The cells were fixed with 4% paraformaldehyde for 15 min. After washing, cells were incubated with 500 μl 50 μg/ml filipin solution for 1 h in the dark. Then the cells were washed twice with PBS, mounted and covered with coverslip. The images were taken using confocal microscope under 360/460 nm.

Western blot

HUVEC were treated with varying concentrations of **15n** for 24 h. Cells were lysed using RIPA buffer and the protein concentration were measured and normalized. After electrophoresis and transfer onto 0.45 μM nitrocellulose membranes, the membranes were blocked with 5% BSA for 1 h and then incubated with primary antibody overnight at 4 °C. Secondary antibody was applied to each membrane for 1 hour. Blots were imaged using

Syngene PXi imaging system after adding chemiluminescent substrate. The following antibodies were used for the assay: AMPKα (1:1,000, cell signaling, #2532s), phosphor-AMPKα (1:1,000, cell signaling #2535s), ACC (1:1,000, cell signaling #3662s), phosphor-ACC (1:1,000, cell signaling, #3661s), mTOR (1:1,000, cell signaling, #2972S), phosphor-mTOR (1:1,000, cell signaling, #9234s), p70 S6 Kinase (1:1,000, santa cruz, #sc-8418), phosphor- p70 S6 Kinase (1:1,000, cell signaling, #3662s), anti-Rabbit IgG (1:10000, GE lifesciences, #NA934V).

Supporting Information: Molecular formula strings (CSV); detail of synthesis procedures; kenetic curve of CYP3A4 enzyme activities; philipin staining of compound **15c**, **15g**; competition assay of itraconazole photoaffinity probe; NMR and HPLC chart of representative compounds

Corresponding Author

*J.O.L.: phone, 410-955-4619; fax, 410-955-4520; e-mail, joliu@jhu.edu

Author Contributions

[II] These authors contributed equally to this work.

Notes

The authors declare no competing financial interest.

Acknowledgment. This work was supported by the National Cancer Institutes (Grant R01CA184103) and the Flight Attendant Medical Research Institute.

Abbreviations:

HUVEC, human umbilical vein endothelial cell; NPC1, Niemann-Pick disease, type C1; VDAC1, voltage-dependent anion channel 1; 14-DM, lanosterol 14-alpha demethylase; mTORC, mammalian target of rapamycin complex; SAR, structure-activity relationship; IC_{50},

half-maximal inhibitory concentration; DMSO, dimethyl sulfoxide; DMF, dimethylformamide; EC_{50}, half-maximal effective concentration; AMPKα, 5' AMP-activated protein kinase α subunit; ATP, adenosine triphosphate; AMP, adenosine monophosphate; CYP3A4, cytochrome P450 3A4; rt, room temperature; THF, tetrahydrofuran; DCM, dichloromethane; TfOH, trifluoromethanesulfonic acid; NaH, sodium hydride; ACC1, acetyl CoA carboxylase 1; S6K, p70 S6 kinase; δ, chemical shifts.

References:

1. Carmeliet, P.; Jain, R. K., Angiogenesis in cancer and other diseases. *Nature* **2000,** *407*, 249-257.
2. Weis, S. M.; Cheresh, D. A., Tumor angiogenesis: molecular pathways and therapeutic targets. *Nat Med* **2011,** *17*, 1359-1370.
3. Chong, C. R.; Xu, J.; Lu, J.; Bhat, S.; Sullivan, D. J., Jr.; Liu, J. O., Inhibition of angiogenesis by the antifungal drug itraconazole. *ACS Chem Biol.* **2007,** *2*, 263-270.
4. Shim, J. S.; Liu, J. O., Recent advances in drug repositioning for the discovery of new anticancer drugs. *Int J Biol Sci.* **2014,** *10*, 654-663.
5. Vanden Bossche, H.; Marichal, P.; Gorrens, J.; Coene, M. C., Biochemical basis for the activity and selectivity of oral antifungal drugs. *Br J Clin Pract Suppl.* **1990,** *71*, 41-46.
6. Lamb, D. C.; Kelly, D. E.; Waterman, M. R.; Stromstedt, M.; Rozman, D.; Kelly, S. L., Characteristics of the heterologously expressed human lanosterol 14alpha-demethylase (other names: P45014DM, CYP51, P45051) and inhibition of the purified human and Candida albicans CYP51 with azole antifungal agents. *Yeast* **1999,** *15*, 755-763.
7. Head, S. A.; Shi, W.; Zhao, L.; Gorshkov, K.; Pasunooti, K.; Chen, Y.; Deng, Z.; Li, R. J.; Shim, J. S.; Tan, W.; Hartung, T.; Zhang, J.; Zhao, Y.; Colombini, M.; Liu, J. O., Antifungal drug itraconazole targets VDAC1 to modulate the AMPK/mTOR signaling axis in endothelial cells. *Proc Natl Acad Sci U S A.* **2015,** *112*, E7276-E7285.
8. Strating, J. R.; van der Linden, L.; Albulescu, L.; Bigay, J.; Arita, M.; Delang, L.; Leyssen, P.; van der Schaar, H. M.; Lanke, K. H.; Thibaut, H. J.; Ulferts, R.; Drin, G.; Schlinck, N.; Wubbolts, R. W.; Sever, N.; Head, S. A.; Liu, J. O.; Beachy, P. A.; De Matteis, M. A.; Shair, M. D.; Olkkonen, V. M.; Neyts, J.; van Kuppeveld, F. J., Itraconazole inhibits enterovirus replication by targeting the oxysterol-binding protein. *Cell Rep.* **2015,** *10*, 600-615.
9. Head, S. A.; Shi, W; Yang, E. J.; Nacev, B.A.; Hong, S.Y.; Pasunooti, K.K.; Li, R.J.; Shim, J.S.; Liu, J.O., Simultaneous targeting of NPC1 and VDAC1 by itraconazole leads to synergistic inhibition of mTOR signaling and angiogenesis. *ACS Chem Biol.* **2017,** *12*, 174-182.
10. Xu, J.; Dang, Y.; Ren, Y. R.; Liu, J. O., Cholesterol trafficking is required for mTOR activation in endothelial cells. *Proc Natl Acad Sci U S A.* **2010,** *107*, 4764-4769.
11. Nacev, B. A.; Grassi, P.; Dell, A.; Haslam, S. M.; Liu, J. O., The antifungal drug itraconazole inhibits vascular endothelial growth factor receptor 2 (VEGFR2) glycosylation, trafficking, and signaling in endothelial cells. *J Biol Chem.* **2011,** *286*, 44045-44056.
12. Antonarakis, E. S.; Heath, E. I.; Smith, D. C.; Rathkopf, D.; Blackford, A. L.; Danila, D. C.; King, S.; Frost, A.; Ajiboye, A. S.; Zhao, M.; Mendonca, J.; Kachhap, S. K.; Rudek, M. A.; Carducci, M. A., Repurposing itraconazole as a treatment for advanced prostate cancer: a noncomparative

randomized phase II trial in men with metastatic castration-resistant prostate cancer. *Oncologist* **2013,** *18*, 163-173.

13. Aftab, B. T.; Dobromilskaya, I.; Liu, J. O.; Rudin, C. M., Itraconazole inhibits angiogenesis and tumor growth in non-Small cell lung cancer. *Cancer Res.* **2011,** *71*, 6764-6772.
14. Rudin, C. M.; Brahmer, J. R.; Juergens, R. A.; Hann, C. L.; Ettinger, D. S.; Sebree, R.; Smith, R.; Aftab, B. T.; Huang, P.; Liu, J. O., Phase 2 study of pemetrexed and itraconazole as second-line therapy for metastatic nonsquamous non-small-cell lung cancer. *J Thorac Oncol.* **2013,** *8*, 619-623.
15. Kim, D. J.; Kim, J.; Spaunhurst, K.; Montoya, J.; Khodosh, R.; Chandra, K.; Fu, T.; Gilliam, A.; Molgo, M.; Beachy, P. A.; Tang, J. Y., Open-label, exploratory phase II trial of oral itraconazole for the treatment of basal cell carcinoma. *J Clin Oncol.* **2014,** *32*, 745-751.
16. Lamb, D. C.; Kelly, D. E.; Baldwin, B. C.; Kelly, S. L., Differential inhibition of human CYP3A4 and Candida albicans CYP51 with azole antifungal agents. *Chem Biol Interact* **2000,** *125*, 165-175.
17. Guengerich, F. P., Cytochrome P-450 3A4: regulation and role in drug metabolism. *Annu Rev Pharmacol Toxicol.* **1999,** *39*, 1-17.
18. van Erp, N. P.; Gelderblom, H.; Guchelaar, H. J., Clinical pharmacokinetics of tyrosine kinase inhibitors. *Cancer Treat Rev* **2009,** *35*, 692-706.
19. Isoherranen, N.; Kunze, K. L.; Allen, K. E.; Nelson, W. L.; Thummel, K. E., Role of itraconazole metabolites in CYP3A4 inhibition. *Drug Metab Dispos.* **2004,** *32*, 1121-1131.
20. Brüggemann, R. J. M.; Alffenaar, J.-W. C.; Blijlevens, N. M. A.; Billaud, E. M.; Kosterink, J. G. W.; Verweij, P. E.; Burger, D. M.; Saravolatz, L. D., Clinical relevance of the pharmacokinetic interactions of azole antifungal drugs with other coadministered agents. *Clin Infect Dis.* **2009,** *48*, 1441-1458.
21. Shi, W.; Nacev, B. A.; Bhat, S.; Liu, J. O., Impact of absolute stereochemistry on the antiangiogenic and antifungal activities of itraconazole. *ACS Med Chem Lett.* **2010,** *1*, 155-159.
22. Shim, J. S.; Li, R. J.; Bumpus, N. N.; Head, S. A.; Kumar Pasunooti, K.; Yang, E. J.; Lv, J.; Shi, W.; Liu, J. O., Divergence of antiangiogenic activity and hepatotoxicity of different stereoisomers of itraconazole. *Clin Cancer Res.* **2016,** *22*, 2709-2720.
23. Shi, W.; Nacev, B. A.; Aftab, B. T.; Head, S.; Rudin, C. M.; Liu, J. O., Itraconazole side chain analogues: structure-activity relationship studies for inhibition of endothelial cell proliferation, vascular endothelial growth factor receptor 2 (VEGFR2) glycosylation, and hedgehog signaling. *J. Med. Chem.* **2011,** *54*, 7363-7374.
24. Pearson, J. T.; Hill, J. J.; Swank, J.; Isoherranen, N.; Kunze, K. L.; Atkins, W. M., Surface plasmon resonance analysis of antifungal azoles binding to CYP3A4 with kinetic resolution of multiple binding orientations. *Biochemistry* **2006,** *45*, 6341-6353.
25. Monk, B. C.; Tomasiak, T. M.; Keniya, M. V.; Huschmann, F. U.; Tyndall, J. D. A.; O'Connell, J. D.; Cannon, R. D.; McDonald, J. G.; Rodriguez, A.; Finer-Moore, J. S.; Stroud, R. M., Architecture of a single membrane spanning cytochrome P450 suggests constraints that orient the catalytic domain relative to a bilayer. *Proc Natl Acad Sci U S A.* **2014,** *111*, 3865-3870.
26. Pace, J. R.; DeBerardinis, A. M.; Sail, V.; Tacheva-Grigorova, S. K.; Chan, K. A.; Tran, R.; Raccuia, D. S.; Wechsler-Reya, R. J.; Hadden, M. K., Repurposing the clinically efficacious antifungal agent itraconazole as an anticancer chemotherapeutic. *J. Med. Chem.* **2016,** *59*, 3635-3649.

27. Bauer, L.; Ferla, S.; Head, S. A.; Bhat, S.; Pasunooti, K. K.; Shi, W. Q.; Albulescu, L.; Liu, J. O.; Brancale, A.; van Kuppeveld, F. J. M.; Strating, J. R. P. M., Structure-activity relationship study of itraconazole, a broad-range inhibitor of picornavirus replication that targets oxysterol-binding protein (OSBP). *Antiviral Res.* **2018,** *156*, 55-63.
28. Choi, I.; Kim, S. Y.; Kim, H.; Kang, N. S.; Bae, M. A.; Yoo, S. E.; Jung, J.; No, K. T., Classification models for CYP450 3A4 inhibitors and non-inhibitors. *Eur J Med Chem.* **2009,** *44*, 2354-2360.
29. Catalan, J.; Menendez, M.; Elguero, J., On the relationships between basicity and acidity in azoles. *Bull. Soc. Chim. Fr.* **1984,** *30,* 30-33
30. Cheng, H.; Zhang, L.; Liu, Y.; Chen, S.; Lu, X.; Zheng, Z.; Zhou, G. C., Design, synthesis and discovery of 5-hydroxyaurone derivatives as growth inhibitors against HUVEC and some cancer cell lines. *Eur J Med Chem.* **2010,** *45*, 5950-5957.
31. Nagata, D.; Mogi, M.; Walsh, K., AMP-activated protein kinase (AMPK) signaling in endothelial cells is essential for angiogenesis in response to hypoxic stress. *J Biol Chem.* **2003,** *278*, 31000-31006.
32. Karar, J.; Maity, A., PI3K/AKT/mTOR pathway in angiogenesis. *Front Mol Neurosci.* **2011,** *4*, 1-8.

Table of Content graphic:

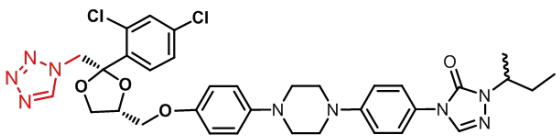

15n
HUVEC IC_{50} = 73nM
CYP3A4 EC_{50} > 20μM
mTOR inhibition
NPC phenotype